Phase equilibria and transformations in adiabatic systems

A. Umantsev
Department of Materials Science and Engineering, The University of Alabama, Birmingham, Alabama 35294-4461

G. B. Olson
Department of Materials Science and Engineering, Northwestern University, Evanston, Illinois 60208-3108
(Received 16 November 1992; revised manuscript received 8 March 1993)

The effect of energy conservation on the decomposition of unstable states is considered for systems undergoing a first-order phase transition with a nonconserved order parameter. Thermodynamic stability analysis shows that in a large enough initially supercooled adiabatic system the mixture of parent and product phases separated by a domain wall is preferred. However, in a small particle a homogeneous phase intermediate between the parent and product phase structures can form. Dynamic analysis of unstable phase decomposition identifies the thermodynamic and kinetic parameters defining different nonlinear dynamic regimes. This includes an interesting regime in which the order parameter is "slaved" to the local temperature. Further evolution of the system has been studied by one-dimensional numerical simulation which reveals three mechanisms of spontaneous domain formation: nonclassical nucleation, continuous modulation, and a hybrid mechanism. Formation of a domain structure is followed by stages of growth and coarsening. Growth can involve heat trapping by the product metastable phase, leading to a transient "overshooting" of the transformed fraction. Coarsening exhibits both coalescence and dissolution and follows a path of sequential period doubling. The results are discussed in terms of application to different first-order phase transformations, including "quasimartensitic" displacive transformation.

PACS number(s): 64.60.−i, 82.20.Mj, 05.70.Fh

I. INTRODUCTION

Kinetics and morphology of transformations in materials are among the most important applications of thermodynamics and statistical mechanics. Usually transitions are studied under conditions of constant temperature and described in terms of nucleation, spinodal decomposition, growth, and coarsening. It is not only the ultimate equilibrium state which is of concern, but also the nature of transformation transients because, given the finite time of processing, the actual structure of materials retains a great deal of its transient morphology.

It is well known that a phase transformation can take place very rapidly. In such a case, it cannot be truly isothermal. Over the past several years much attention has been given to this problem under conditions of conservation of energy, which can be especially important when the transformation order parameter is not itself a conserved quantity. Langer [1] and Metiu, Kitahara, and Ross [2] showed that depending upon the nature of the order parameter, its evolution in the framework of the continuum theory is governed by equations of different types: the Cahn-Hilliard equation [3], if this parameter obeys a conservation law, or the relaxation equation if it does not. The latter case is addressed in this paper.

The first attempt to describe the conservation of energy was made by Halperin, Hohenberg, and Ma [4] and gave rise to the so-called "model C," which utilizes the Cahn-Hilliard-type equation for energy density evolution. Recently an analogous equation for the same purposes was employed by Penrose and Fife [5]. Another attempt has been made to describe energy redistribution by the diffusion equation for the entropy density [6]. The most widespread is the so-called "phase-field" model, introduced first by Caginalp [7] and Collins and Levine [8], which describes the conservation of energy by an inhomogeneous diffusion-type equation for temperature, with the constant density of instantaneous heat sources equal to the latent heat of the transformation. All the equations were proposed on a semiintuitive basis and are not exact. Umantsev and Roitburd [9] developed a thermodynamically consistent approach to this problem and *derived* the evolution equation for the energy of a nonlocal medium.

Being cooled below the equilibrium point the high-symmetry α phase becomes capable of a transition to the low-symmetry β phase (e.g., solidification or martensitic transformation). The conservation law can lead to first-order transformation kinetics controlled by the conserving quantity [10]. However, the dynamic equations employed for such cases [10] cannot describe the transformation with energy being the conserved thermodynamic variable. Fife and Gill [11] studied a problem of energy conservation in the framework of the phase-field model and showed a possibility of transformation through a fine-grained intermediate structure. Umantsev and Olson [12] studied the linear and weakly nonlinear dynamical behavior of the nonconserved order parameter in the presence of energy conservation and found that the coupling between these two modes is described by the mixed partial derivative of the free energy with respect to the order parameter and temperature. Also they found that in the case of sufficiently strong coupling, early (but not

necessarily initial) stages of the order-parameter evolution are described by the nonlinear Cahn-Hilliard equation, which corresponds to conservation of this parameter despite its intrinsically nonconserved nature.

Asymptotic regimes (growth stages) of this process in an infinite one-dimensional (1D) system were studied many times in the framework of a free-boundary problem, which is the sharp interface limit of the continuum theory. Depending upon the supercooling of the α phase three different regimes exist: (a) for supercoolings less than critical, the diffusion controlled Stefan regime applies with the front velocity decaying as the square root of time, equilibrium temperature at the front and an expanding thermal field ahead of it; (b) for supercoolings greater than critical, the kinetic controlled stationary regime of the adiabatic transformation with the product phase temperature below the equilibrium point; and (c) the intemrediate regime with the front velocity decaying as the cubic root of time obtains for the critical supercooling [13]. However, in the continuum theory there exist stationary solutions for supercoolings less than critical [9,14,15]. This means that the β phase, appearing as a result of such transformation, is superheated above the equilibrium temperature. This effect, called heat trapping, consists of adiabatic absorption by the front of the heat released by the transition from the unstable or metastable α state so that the product phase appears to be metastable (in the isothermal sense). It exists only in a bounded interval of supercoolings, with the low limit depending upon the thermal diffusivity and is absent if the thermal diffusivity is above the critical value [9,14]. The heat-trapping regime is due to heat diffusion inside the interfacial transition region and is analogous to the partitionless solidification of alloys (solute trapping), which results in the appearance of crystalline alloys with solute in excess of equilibrium solubility [16].

In the present paper we examine the general effect of energy conservation on the first-order-transformation process in unstable systems with a nonconserved order parameter. We aim to explore a thermodynamically rigorous model and understand also the *global* equilibrium of a system brought initially to a certain degree of supercooling and then thermally isolated. Such an initial state can also be achieved in a thermally isolated system by application or release of an interacting field. For an isothermal system the question of the global equilibrium can be resolved easily from the consideration of the free energies of the two phases: regardless of its size the system ends up in a homogeneous phase with the lowest possible free energy. Obviously, in the adiabatic system the tranditional picture of two intersecting convex free energies as functions of temperature is no longer valid for determining the global equilibrium. The local thermodynamic stability analysis of the unbounded adiabatic system [14,17] shows that homogeneous and even inhomogeneous states which are absolutely unstable under isothermal conditions may be stable under adiabatic conditions. At first glance a supercooled and then thermally isolated homogeneous system must end up at a mixture of the two phases at the equilibrium temperature. Yet it is not necessarily the case for a system of finite size.

There are a number of physical examples which can be described by this type of theory. In the case of a displacive structural transformation where the order parameter is a strain, it has been suggested [18] that a first-order transition might occur by a continuous strain-modulation mechanism controlled by heat transfer; termed *quasimartensitic* transformation, this constitutes an alternative to *martensitic* nucleation and growth. The problem of interest can also be relevant to magnetic and superconducting first-order transitions with magnetization and wave function of the superconducting electrons, respectively, as the order parameter, or liquid crystals which are characterized by a certain degree of orientational order, if the cumulative heat release of the transition is essential. There also have been several attempts to build a continuum theory of crystallization with the order parameter related to the different symmetries of liquid and crystalline phases. The results also can be used to discuss the order-disorder transition in solids with concentration field replacing the temperature field.

The paper is organized as follows. Section II is devoted to the global thermodynamic stability of all equilibrium states in a thermally insulated system, determining the ultimate product of the transformation. In Sec. III we analyze the initial and late stages of the transition leading to domain structure formation. In Sec. IV we take advantage of the method of direct numerical simulation and discuss the results in Sec. V, which is followed by the conclusions in Sec. VI.

II. EQUILIBRIUM STATE DIAGRAM OF AN ADIABATICALLY INSULATED SYSTEM

The continuum theory of phase transitions assumes that the state of a system at a given time t, in addition to temperature T, and pressure, must be described by one more function of the position vector $\mathbf{x}$. We shall call it the order-parameter field (OPF) $\xi(\mathbf{x},t)$. The nonequilibrium Gibbs free energy (effective Hamiltonian) Φ of the medium capable of undergoing a first-order phase transition can be written in the form of a functional:

$$\Phi=\int \hat{\varphi}\, d^3x \ , \quad \hat{\varphi}=\varphi(\xi,T,b)+\frac{\kappa}{2}(\nabla\xi)^2 \ , \tag{2.1}$$

where the free energy per unit volume $\hat{\varphi}$ is the differential expression in the Landau form with the square gradient approximation for the nonlocal part [19]. The parameter κ characterizes the nonlocal properties of the medium (interactions between neighboring areas) and is assumed here to be constant. To stabilize a homogeneous state κ must be positive. The homogeneous part of the free energy density

$$\varphi(\xi,T,b)=\varphi_\alpha(T)+\Delta\varphi(\xi,T)-b\xi \tag{2.2}$$

consists of the Gibbs free energy $\varphi_\alpha(T)$ of the high-temperature (disordered) state $\alpha=\{\xi_\alpha=0,T\}$, the double-well free-energy increment $\Delta\varphi(\xi,T)$, and the generalized work term, where b is the outer biasing field conjugate to the OPF of the problem. The latter is the magnetic field for ferromagnetic transformations and stress for displacive structural transformations in solids. The

free-energy increment $\Delta\varphi(\xi,T)$ should determine the isothermal transformation from the α state to the low-temperature (ordered) state $\beta=\{\xi_\beta>\xi_\alpha,T\}$, separated from the α state by the unstable equilibrium state $\gamma=\{\xi_\alpha<\xi_\gamma<\xi_\beta,T\}$, corresponding to the free-energy crest (Fig. 1). The equilibrium point T_0 of α and β states is defined so that $\Delta\varphi(\xi_\beta,T_0)=0$. The isothermal stability of homogeneous equilibrium states (HES's) is known to be governed by the isothermal modulus $\bar{\varphi}_{\xi\xi}$:

$$\bar{\varphi}_{\xi\xi}\geq 0 \tag{2.3}$$

(functions with a bar should be taken at equilibrium). Locally stable HES's we shall call *phases.*

If adiabatic conditions are maintained for a system (microcanonical ensemble) then its energy W (or enthalpy if pressure is constant), which can be written as a functional, is conserved, i.e.,

$$W\equiv\int\left[w(\xi,T,b)+\frac{\kappa}{2}(\nabla\xi)^2\right]d^3x=\text{const}\ . \tag{2.4}$$

There are no conservation constraints on the OPF because the latter is assumed to be nonconserved. The entropy functional takes on a maximum at the stable equilibrium states [20]:

$$S\equiv\int s(\xi,T,b)d^3x\rightarrow\text{maximum}\ , \tag{2.5}$$

where $w=\varphi-T(\partial\varphi/\partial T)_\xi$ and $s=-(\partial\varphi/\partial T)_\xi$ are the energy and entropy per unit volume, respectively. Negative entropy is a Lyapunov functional of the problem. Such a system has the same equilibrium states as that under isothermal conditions. They are represented by solutions of the equation

$$\kappa\nabla^2\xi=\frac{\partial\varphi(\xi,T,b)}{\partial\xi}\ ,\quad T=\text{const}\ . \tag{2.6}$$

However, adiabatic conditions can change stabilities of these states [14,17], and a uniform isothermally unstable

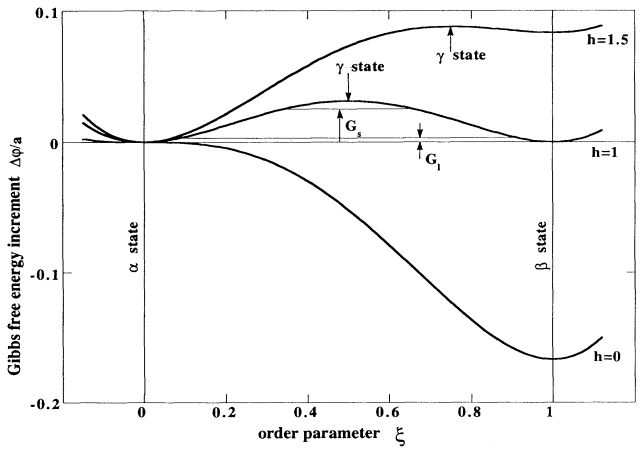

FIG. 1. Gibbs free energy increment $\Delta\varphi/a$ as a function of the order parameter ξ at different scaled temperatures h. Two different values of the constant G that correspond to monotonic solutions of Eq. (2.8) at the equilibrium temperature in large (G_l) and small (G_s) systems are shown.

($\bar{\varphi}_{\xi\xi}<0$) equilibrium state (i.e., $\gamma=\{\xi_\gamma,T\}$) can be thermodynamically stable under adiabatic conditions if the adiabatic modulus $(\bar{\varphi}_{\xi\xi}-\bar{\varphi}^2_{\xi T}/\bar{\varphi}_{TT})$ of this state is positive—the "adiabatic state" (AS). With the help of the modulus M,

$$M\equiv\frac{\bar{\varphi}^2_{\xi T}}{\bar{\varphi}_{\xi\xi}\bar{\varphi}_{TT}}\ , \tag{2.7}$$

which represents thermodynamic properties of the HES, this thermodynamic criterion can be expressed as follows: $M<0$ or $M>1$, while isothermal stability corresponds to the case $M<0$ only.

Besides homogeneous solutions, Eq. (2.6) is known to have bounded inhomogeneous solutions—inhomogeneous equilibrium states (IES's). In the 1D case they break into three classes: periodic, solitonlike (critical nucleus), and kinklike (domain wall) solutions [21,1,22]. IES's for all temperatures are isothermally unstable except for the domain wall in the infinite system at the specific temperature T_0 (the equilibrium point) [21,1,23], which is a reflection of the Gibbs phase rule. Adiabatic insulation can also change stability conditions of these states and the critical nucleus or a periodic solution can be thermodynamically stable, if the adiabatic modulus $(\bar{\varphi}_{\xi\xi}-\bar{\varphi}^2_{\xi T}/\bar{\varphi}_{TT})$ is positive at all points of the system [14]. Hence one can say that the adiabatic system is "more stable" than the isothermal one [24]. It has been also demonstrated [14] that, except for the solutions of Eq. (2.6), the adiabatic system (2.4) and (2.5) has an equilibrium state which is inhomogeneous in OPF and temperature but homogeneous in entropy density. This state is thermodynamically unstable and represents a saddle point.

The problem addressed in this paper is a disintegration of unstable and metastable equilibrium disordered states under constraint of adiabatic insulation which is guaranteed by the Neumann-type boundary conditions: $\partial_n\xi=\partial_n T=0$, where ∂_n denotes differentiation normal to the boundary. In the 1D case a system of finite size occupies the closed interval $0\leq x\leq X_0\leq\infty$. The influence of pressure is not the issue of the present work, so it will be considered invariable. The influence of the outer biasing field b was addressed in [12] and below only the case $b=0$ is considered.

The transformation starts from the parent state $\alpha=\{\xi_\alpha,T_\alpha\}$, where temperature $T_\alpha<T_0$ characterizes the initial degree of supercooling, and may arrive at one of the uniform equilibrium states: product $\beta=\{\xi_\beta,T_\beta\}$ which is globally stable if its temperature $T_\beta<T_0$, or at the state $\gamma=\{\xi_\gamma,T_\gamma\}$, which may be stable either *only* thermodynamically (AS) if $\xi_\alpha<\xi_\gamma<\xi_\beta$ or even dynamically (linearly stable) if $\xi_\gamma<\xi_\alpha$ or $\xi_\gamma>\xi_\beta$. Starting from the unstable or metastable α state the system may also arrive at one of the IES, because the thermodynamic criterion of the global stability, Eq. (2.5), requires that the system generates the state which has more entropy than any other state with the same energy, Eq. (2.4). Simply stated, the system may break down into domains if the entropy of this state is greater than that of all possible HES's. For this reason we shall calculate *entropies of*

different IES's versus their energies, which will enable us to build an equilibrium state diagram of our system. It is possible to implement this program by analyzing dynamic stabilities of different IES's existing in the system. However, this mathematical problem is not solves as yet and we take a more physical approach.

To study the IES's we multiply all terms of Eq. (2.6) in the 1D case by $d\xi/dx$ and integrate them with respect to x. This yields

$$\frac{\kappa}{2}\left[\frac{d\xi}{dx}\right]^2=\Delta\varphi(\xi,T)-G \ . \tag{2.8}$$

For the existence of bounded solutions of this equation an arbitrary constant G must satisfy the condition

$$\max[0,\Delta\varphi(\xi_\beta,T)]\le G\le\Delta\varphi(\xi_\gamma,T) \ . \tag{2.9}$$

Under this condition the equation $\Delta\varphi(\xi,T)=G$ has four real roots ξ_i, $i=1,2,3,4$, while two of them are between ξ_α and ξ_β: $\xi_\alpha\le\xi_1<\xi_2\le\xi_\beta$. Suppose we determine an axis x so that $\xi(0)=\xi_2$. Then the bounded solution of Eq. (2.8) takes the form [22]

$$x=\sqrt{\kappa/2}\int_{\xi\ge\xi_1}^{\xi_2}\frac{d\tilde{\xi}}{\sqrt{\Delta\varphi(\tilde{\xi},T)-G}} \ . \tag{2.10}$$

To characterize the periodic solutions we introduce the half-period P so that $\xi(P)=\xi_1$ and the product phase fraction f

$$f=\frac{1}{P}\int_0^P\xi\,dx=-\frac{1}{P}\int_{\xi_1}^{\xi_2}\frac{\xi d\xi}{d\xi/dx} \ , \quad P=-\int_{\xi_1}^{\xi_2}\frac{d\xi}{d\xi/dx} \ , \tag{2.11}$$

where $0<f<1$ according to the definition. Due to the Neumann-type boundary conditions

$$\frac{d\xi}{dx}=\frac{dT}{dx}=0 \quad \text{for } x=0 \ , \ x=X_0 \tag{2.12}$$

the aspect ratio of the state $N=X_0/P$, the number of the half-periods, is a monotonic function of the constant G.

Now we shall define the free energy of the state $\Delta\Phi$ per unit area in excess to the parent phase free energy $\varphi_\alpha(T)X_0$:

$$\begin{aligned}\Delta\Phi&=\int_0^{X_0}\left[\kappa\left[\frac{d\xi}{dx}\right]^2+G\right]dx\\&=N\sqrt{2\kappa}\int_{\xi_1}^{\xi_2}\sqrt{\Delta\varphi(\xi,T)-G}\,d\xi+X_0G \ ,\end{aligned} \tag{2.13}$$

where Eqs. (2.1), (2.2), and (2.8) were used, and the integration is over the whole volume occupied by the system. The domain wall at the equilibrium point ($N=1, G=0, X_0\to\infty$) can be characterized by the excess free energy (the surface free energy or surface tension):

$$\sigma\equiv\int_{-\infty}^{+\infty}[\hat{\varphi}-\varphi_\alpha(T_0)]dx=\kappa\int_{-\infty}^{+\infty}\left[\frac{d\xi}{dx}\right]^2dx \tag{2.14a}$$

and the width of the transition region

$$l_w\equiv\frac{\xi_\beta-\xi_\alpha}{\max|\nabla\xi|}=\sqrt{\kappa/2}\frac{\xi_\beta-\xi_\alpha}{\sqrt{\Delta\varphi(\xi_\gamma,T_0)}} \ . \tag{2.14b}$$

For the continuum approach to be applicable the interfacial width should be much larger than interatomic spacing.

The excess entropy ΔS of IES's can be determined as follows:

$$\begin{aligned}\Delta S&\equiv-\int_0^{X_0}\left[\frac{\partial\Delta\varphi}{\partial T}\right]_\xi dx\\&=-N\sqrt{2\kappa}\int_{\xi_1}^{\xi_2}\left[\frac{\partial}{\partial T}\sqrt{\Delta\varphi-G}\right]_\xi d\xi \ .\end{aligned} \tag{2.15}$$

Analyzing this expression one can see that being in the inhomogeneous state the system tends to decrease the number of half-periods N until one is left and to form a monotonic state of the unit aspect ratio: $N=1$ ($P=X_0$) [24], which corresponds to the complete phase separation.

Differentiating $\Delta\Phi$ in Eq. (2.13) with respect to temperture, taking into account that limits ξ_i are roots of the equation $\Delta\varphi(\xi_i,T)=G$, hence functions of temperature, and comparing with the expression (2.15) we obtain

$$\Delta S=-\frac{d\Delta\Phi}{dT} \ , \tag{2.16}$$

which means that the excess entropy and free energy of IES's are connected by the usual thermodynamic expression.

Being supercooled below the equilibrium point T_0 the α state becomes unstable against the IES formation. Assuming that the specific heat $C=-Td^2\varphi_\alpha/dT^2$ of the α state is constant in the temperature range of transformation, the condition of conservation of energy (2.4) yields

$$T_\alpha=T+\frac{\Delta W}{CX_0} \ , \tag{2.17}$$

where the excess internal energy of the IES at the temperature T can be written as follows:

$$\Delta W=\Delta\Phi-T\frac{d\Delta\Phi}{dT} \ . \tag{2.18}$$

According to the thermodynamic criterion, IES's branch off the line of homogeneous α states at the bifurcation point where their entropies are equal:

$$s_\alpha(T_\alpha)=s_\alpha(T)+\frac{\Delta S(T)}{X_0} \ .$$

Expanding entropy density s_α of the α state in temperature and utilizing (2.17) we obtain the expression for the bifurcation point:

$$X_0=\frac{(\Delta W)^2}{2CT\Delta\Phi} \ . \tag{2.19}$$

This expression, together with Eq. (2.17), describes the boundary of the global stability of the homogeneous α state so that for temperatures greater than T_α from Eqs. (2.17) and (2.19) this state is absolutely stable, although supercooled, while for temperatures less than that T_α the α state should transfer to the IES. The apperance of inhomogeneous states on the equilibrium state diagram of an adiabatically insulated sytem brings also a significant

size dependence [the criterion of bifuraction, Eqs. (2.17), and (2.19), depends upon X_0], while the equilibrium state diagram of an isothermal system is absolutely independent of its size (if the Neumann-type boundary conditions for the OPF are imposed).

To accomplish the thermodynamic description of the system we now adopt a double-well free-energy increment of the form [14]

$$\Delta\varphi(\xi,h)=a\left[\tfrac{1}{2}\omega^2(\xi)+\Omega\Delta h\nu(\xi)\right],\quad \omega(\xi)=\xi(1-\xi),$$
$$\nu(\xi)=\xi^2(3-2\xi),\quad \Omega=\int_0^1\omega(\xi)d\xi=\tfrac{1}{6},$$
$$\Delta h=h-1=\frac{T-T_0}{ET_0},\quad h=\frac{T-T_\alpha^*}{ET_0},\quad E=\frac{\Omega a}{L},\tag{2.20}$$
$$h(T_\alpha^*)=0,\quad h(T_0)=1,\quad h(T_\beta^*)=2,$$

where the constant a scales the free-energy increment and defines the barrier height of the free-energy density at equilibrium: $\Delta\varphi(\xi_\gamma,T_0)=a/32$, L is the latent heat of the reaction, T_i^* is the critical point of instability (such as a spinodal point) of the disordered ($i=\alpha$) or ordered ($i=\beta$) phases, Δh is the normalized temperature calculated from the equilibrium point T_0, and h is the normalized temperature calculated from the instability point T_α^*. In Fig. 1 the increment $\Delta\varphi$ is represented as a function of ξ for different scaled temperatures h. In Fig. 2 HES's [homogeneous solutions of Eq. (2.6)] $\alpha=\{\xi_\alpha=0,h\}$, $\beta=\{\xi_\beta=1,h\}$, and $\gamma=\{\xi_\gamma,h=2\xi_\gamma\}$ are depicted as solid lines in the plane (ξ,h). Heavy lines in Fig. 2 stand for the phases. The instability points T_i^* are intersections of two equilibrium lines. Together with HES's in Fig. 2 are depicted the lines of states with constant energy (dashed lines):

$$w(\xi,\Delta h)=a\left[\frac{\Omega}{Q}\Delta h-\frac{\Omega}{E}\nu(\xi)+\tfrac{1}{2}\omega^2(\xi)\right]=\text{const},$$
$$Q=\frac{L}{CT_0}\tag{2.21}$$

for two different values of the parameter Q, which is the ratio of the two temperature scales of the transformation: temperature increase due to heat liberation and the equilibrium point temperature. Entropy densities of these states are

$$s(\xi,\Delta h)=C[\ln(1+E\Delta h)-Q\nu(\xi)],\tag{2.22}$$

where the state $\alpha=\{\xi_\alpha=0,h_\alpha=1\}$ at the equilibrium point is the reference state for energy and entropy density calculations.

For the temperature of the β state after transformation T_β, the constraint of energy conservation (2.4) yields $T_\beta=T_\alpha+L/C$ or in the scaled units

$$h_\beta=h_\alpha+\frac{1}{r},\quad r=\frac{E}{Q}=\Omega\frac{aCT_0}{L^2}.\tag{2.23}$$

Parameter r is the relative measure of three different energy scales $\Delta\varphi(\xi_\gamma,T_0)$, CT_0, and L existing in the system. From Eqs. (2.21) and (2.22) one can obtain expressions for the entropy densities of the α states

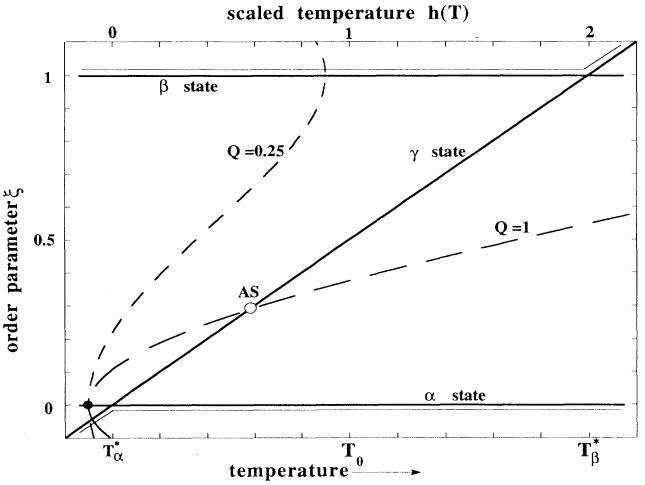

FIG. 2. Equilibrium diagram of the homogeneous states: the solid lines represent equilbrium states, the heavy lines represent their locally stable parts (phases), and the dashed lines stand for level lines of constant energy for the systems with $E=0.25$ and different values of the parameter Q. Open circle, the adiabatic state; solid circle, the initial state for numerical simulation.

$$s_\alpha=C\ln(1-Q\Delta\theta)\tag{2.24}$$

and the β states

$$s_\beta=C[\ln(1-Q\Delta\theta+Q)-Q]\tag{2.25}$$

as functions of the dimensionless initial supercooling of the α state:

$$\Delta\theta=\frac{T_0-T_\alpha}{L/C}=r(1-h_\alpha),\tag{2.26}$$

which is a measure of the total energy of the system:

$$W=-\Delta\theta LX_0.\tag{2.27}$$

For small supercoolings $s_\alpha>s_\beta$, for $\Delta\theta$ close to one, $s_\beta>s_\alpha$, and for $\Delta\theta_{\alpha\beta}=Q^{-1}-(e^Q-1)^{-1}$, the entropy of the product state is equal to the entropy of the parent state from which it emerges [14,25].

Also Eqs. (2.21)and (2.22) yield an implicit expression for the γ-state entropy density vs supercooling:

$$s_\gamma=C\{\ln[1-E(1-2\xi)]-Q\nu(\xi)\},\tag{2.28a}$$
$$\Delta\theta=\nu(\xi)-\frac{E}{2\Omega}\omega^2(\xi)+r(1-2\xi).\tag{2.28b}$$

An analysis of Eqs. (2.24) and (2.28) shows that for the system with $r<3/4$ [the condition of the AS existence, see Eq. (3.14) of [14]] there exists a bifurcation point $\Delta\theta_{\alpha\gamma}$ wher entropies of the α and γ states are equal. For supercoolings larger than $\Delta\theta_{\alpha\gamma}$ the γ state is preferable (AS).

The temperature of the IES after transformation in a *large* system should be close to T_0. So, for the periodic IES $\mathcal{I}=\{f,\Delta h\}$ with small Δh and $N=1$ [and small constant G of Eq. (2.8), see condition (2.9) and Fig. 1] one can obtain the approximation

$$\frac{2\Delta\varphi}{a}\approx\begin{cases}\xi^2\ , & \xi\rightarrow\xi_1\\ [\xi(1-\xi)]^2\ , & \xi_1<\xi<\xi_2\\ (1-\xi)^2+2\Omega\Delta h\ , & \xi\rightarrow\xi_2\ ,\end{cases} \tag{2.29}$$

$$\frac{d\xi}{dx}\approx\pm\frac{\omega}{\delta}\ ,\quad \delta=\sqrt{\kappa/a}\ , \tag{2.30}$$

$$fX_0\approx\int_0^P \nu\,dx\ , \tag{2.31}$$

where δ is the characteristic length scale. In fact, the $\mathcal{I}=\{f,\Delta h\}$, described by Eqs. (2.29)–(2.31), is a two-phase state where product and parent phases are separated by a domain wall, which has the well-known form of a hyperbolic tangent and is characterized by the width of a transition region: $l_w=4\delta$, Eq. (2.14b). The excess free energy of this IES takes the form

$$\Delta\Phi_w=\int_0^{X_0}\left[\frac{a}{2}\omega^2(\xi)+\frac{\kappa}{2}\left[\frac{d\xi}{dx}\right]^2+\Omega a\,\Delta h\,\nu(\xi)\right]dx$$

$$\approx\sigma+\Omega a\,\Delta h f X_0\ ,\quad \sigma=\Omega\sqrt{\kappa a}\ . \tag{2.32}$$

The surface tension introduces another (capillary) length scale σ/L to the problem which, as can be seen from Eqs. (2.20), (2.30), and (2.32), relates to the scale δ as follows:

$$\frac{T_0-T_\alpha^*}{T_0}\equiv E=\frac{\sigma/L}{\delta}\ . \tag{2.33}$$

Utilizing (2.32) for (2.16) and (2.18) we can express the excess entropy and energy of this IES:

$$\Delta S_w=-\frac{L}{T_0}X_0 f\ , \tag{2.34}$$

$$\Delta W_w=\sigma-LX_0 f\ . \tag{2.35}$$

The condition of energy conservation, Eq. (2.17), together with Eqs. (2.21), (2.33), and (2.35), yields the relation for the fraction of this state:

$$f=\Delta\theta+\frac{E}{\Lambda}+r\Delta h\ . \tag{2.36}$$

Here $\Lambda\equiv X_0/\delta$ is the dimensionless size of the system. The first term of this relation is analogous to the lever rule in alloy solidification, the second one is the surface tension contribution which is present even in the sharp interface limit due to the surface-to-volume ratio, and the thrid term reflects a small deviation of temperature from the equilibrium point and occurs in the continuum approach only. Finally from Eqs. (2.34) and (2.36) we obtain the expression for the average entropy of the $\mathcal{I}=\{f,\Delta h\}$:

$$\frac{S_w}{X_0}=s_\alpha(\Delta h)+\frac{\Delta S_w}{X_0}=C\ln(1+E\Delta h)$$

$$-\frac{L}{T_0}\left[\Delta\theta+r\Delta h+\frac{E}{\Lambda}\right]\ , \tag{2.37}$$

which shows that for the fixed initial supercooling $\Delta\theta$: $S_w\sim-(\Delta h)^2$, i.e., the IES temperature after transformtion tends to T_0. This confirms our assumption of small Δh. However, Δh is not identically zero, which, according to Eqs. (2.10) and (2.11), would require practically the same transformation fraction (50%) for different values of the initial supercoolings. To determine the temperature of this $\mathcal{I}=\{f,\Delta h\}$ we utilize the approximation (2.29) for Eq. (2.11) which yields the relations

$$\Lambda f\approx-\ln(1-\xi_2)\ ,\quad \Lambda\approx-\ln\xi_1-\ln(1-\xi_2)\ .$$

Excluding ξ_1 and ξ_2 we obtain the equation for the deviation of temperature Δh from the equilibrium point for the $\mathcal{I}=\{f,\Delta h\}$:

$$\Omega\Delta h=\sinh(f-\tfrac{1}{2})\exp(-\Lambda)\ , \tag{2.38}$$

which shows that Δh is exponentially small for large Λ [26].

Applying Eqs. (2.32)–(2.38) to Eqs. (2.17) and (2.19) one can obtain the bifurcational value of the supercooling of a particle of size Λ, when the two-phase state with a domain wall branches off the α phase:

$$\Delta\theta_{\alpha w}=\sqrt{2r/\Lambda}\ . \tag{2.39}$$

Equilibrating the average entropy of this $\mathcal{I}=\{f,\Delta h\}$ [Eq. (2.37)], with the entropy density of the α state [Eq. (2.24)] yields the same expression (2.39). Comparing the average entropy of the IES, Eq. (2.37), with the entropy density of the β state, Eq. (2.25), yields the bifurcational value of the supercooling of a particle of size Λ, when the two-phase state with a domain wall branches off the β phase:

$$\Delta\theta_{\beta w}=1-\sqrt{2r/\Lambda}\ . \tag{2.40}$$

Thus Eqs. (2.39) and (2.40) constitute, respectively, the left and right boundaries of global stability of two-phase states.

The IES after transformation is described satisfactorily by Eqs. (2.36)–(2.40) only if the amount of the product phase is sufficient to generate a domain wall. The product phase can sustain a domain wall if the width of the latter fX_0 is greater than that of a transition region (domain wall): $l_w=4\delta$. As the transformation fraction for the bifurcational value of supercooling is $\sqrt{2r/\Lambda}$ [Eqs. (2.36) and (2.39)], this criterion takes the form $\Lambda\geq 8/r$. The transformation in a *smaller* particle close to the left boundary of stability, Eq. (2.39), is better represented by the critical nucleus solution, despite a small inconsistency in the boundry condition (2.12) at one of the boundaries (the order-parameter gradient is small but nonvanishing). The critical nucleus corresponds to the case $\Delta h<0$ and $G=0$, which yields for the OPF

$$\xi_1=0\ ,\quad \xi_2\equiv\xi_c=\tfrac{1}{3}[2+h-\sqrt{(1-h)(4-h)}\,)]\ . \tag{2.41}$$

The half-width of this state l_c^+ can be characterized by the distance between the maximal point $\xi(0)=\xi_c$ and the point of inflection which, according to Eq. (2.6), corresponds to the γ state: $\xi(l_c^+)=\xi_\gamma=h/2$. Then Eq. (2.10) yields

$$\frac{l_c^+}{\delta}=\int_{\xi_\gamma}^{\xi_c}\frac{d\xi}{\xi\sqrt{h-\frac{2}{3}(h+2)\xi+\xi^2}}$$

$$=\frac{1}{\sqrt{h}}\ln\frac{\sqrt{3}+\sqrt{4-h}}{\sqrt{1-h}}\rightarrow\begin{cases}\dfrac{\ln(2+\sqrt{3})}{\sqrt{h}}\ , & h\rightarrow 0+0\\ \ln\dfrac{2\sqrt{3}}{\sqrt{1-h}}\ , & h\rightarrow 1-0\ .\end{cases}\tag{2.42}$$

Contrary to the classical and quasiclassical [27] considerations, the half-width l_c^+ of the 1D critical nucleus (critical platelet) is nonzero, of the order of δ, and even diverges when the temperature approaches the equilibrium point from below ($h\rightarrow 1-0$). However, this divergence is logarithmic, while the critical radii of the 2D and 3D classical and quasiclasical nuclei diverge linearly in (T_0-T) or Δh. It is interesting to note that l_c^+ also diverges as $l_c^+\sim\delta/\sqrt{h}$ when the temperature approaches the instability point T_α^* from above ($h\rightarrow 0+0$). This is reflected in Fig. 3, where l_c^+/δ is depicted as a function of h [thick line, Eq. (2.42)] together with the order-parameter value at the center ξ_c [dashed line, Eq. (2.41)], which is monotonically decaying from $\xi_c=1$ at $h=1$ to $\xi_c=0$ at $h=0$. It will be helpful to compare l_c^+ with the half-width of the domain wall $\frac{1}{2}l_w=2\delta$. In the vicinity of the equilibrium point ($h\rightarrow 1-0$) the critical excitation with the half-width l_c^+, Eq. (2.42), represents a classical critical nucleus because it is much thicker than the interface and the order parameter at the center $\xi_c\rightarrow 1$. In the vicinity of the instability point ($h\rightarrow 0+0$) $l_c^+\gg\frac{1}{2}l_w$ also. However, the critical excitation has strongly nonclassical nature [28], because $\xi_c\rightarrow 0$ here.

According to the definition (2.11), the transformation fraction f of this state takes the form

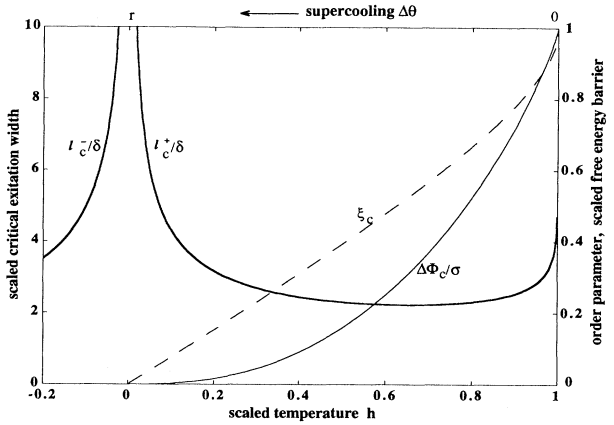

FIG. 3. Parameters of the 1D critical nucleus: scaled half-width l_c^+/δ (thick line), free-energy barrier $\Delta\Phi_c/\sigma$ (solid line), and order-parameter value ξ_c at the center (dashed line) vs scaled temperature h. For $h<0$ the thick line represents the scaled half-period l_c^-/δ of the critical excitation.

$$\Lambda f\approx\delta\int_0^{\xi_c}\frac{\xi\,d\xi}{|d\xi/dx|}=\int_0^{\xi_c}\frac{d\xi}{\sqrt{h-2(h+2)\xi/3+\xi^2}}$$

$$=\ln\frac{\sqrt{(1-h)(4-h)}}{(1-\sqrt{h})(2-\sqrt{h})}$$

$$\rightarrow\begin{cases}\sqrt{h}\ , & h\rightarrow 0+0\\ \ln\dfrac{2\sqrt{3}}{\sqrt{1-h}}\ , & h\rightarrow 1-0\ .\end{cases}\tag{2.43}$$

A comparison of Eqs. (2.42) and (2.43) shows that for $h\rightarrow 0+0$, $f\rightarrow 0$, although $l_c^+\rightarrow\infty$. When $h\rightarrow 1-0$ l_c^+ diverges also and $f\rightarrow l_c^+/X_0$. The latter means that the "critical nucleus" tends to the solution of the domain-wall type. For the critical nucleus ($N=1$, $G=0$, $X_0\rightarrow+\infty$) the formula (2.13) applies also:

$$\frac{\Delta\Phi_c}{\sigma}=\frac{\sqrt{2\kappa}}{\sigma}\int_0^{\xi_c}\sqrt{\Delta\varphi(\xi,h)}\,d\xi=\frac{1}{9}\left[3\sqrt{h}\,(4-2h+h^2)+\frac{1}{2}(2+h)(1-h)(4-h)\ln\frac{(1-\sqrt{h})(2-\sqrt{h})}{(1+\sqrt{h})(2+\sqrt{h})}\right]$$

$$\rightarrow\begin{cases}0.9h^{5/2}+O(h^{7/2})\ , & h\rightarrow 0+0\\ 1-(1-h)\ln\dfrac{2\sqrt{3}}{\sqrt{1-h}}\ , & h\rightarrow 1-0\ .\end{cases}\tag{2.44}$$

The excess free energy (nucleation barrier) is the free energy barrier in the functional space of inhomogeneous states and is also depicted in Fig. 3 (solid line). In the limit $h\rightarrow 1-0$ ($T\rightarrow T_0$ from below) the excess free energy $\Delta\Phi_c$, Eq. (2.44), can be separated into surface (first term) and bulk (second term) contributions and Eq. (2.42) gives the correct value of the product phase bulk width. In the limit $h\rightarrow 0+0$ ($T\rightarrow T_\alpha^*$ from above) the free-energy barrier decays rapidly, and these contributions cannot be separated because bulk is indistinguishable from the surface. Utilizing expression (2.44) for Eqs. (2.17) and (2.19) one can obtain the bifurcational value of the supercooling $\Delta\theta_{\alpha c}$ when the critical nucleus solution branches off the α phase.

Transformation in a small particle close to the right boundary, Eq. (2.40), finishes in the IES, which may be characterized by the solution of Eq. (2.8) with $\Delta h>0$, $G=\Delta\varphi(\xi_\beta,h)$ and consists of totally transformed β state minus the critical nucleus (the "critical hole" solution). Changing variables to $y=X_0-x$, $\eta(y)=1-\xi(x)$, $\Delta\tilde{h}=-\Delta h$ one can show that

$$\Delta\Phi_h=\Omega a\,\Delta h X_0+\Delta\Phi_c(1-\Delta h)\ ,\tag{2.45}$$

which, together with Eqs. (2.17) and (2.19), yields the bi-

furcational value of the supercooling $\Delta\theta_{\beta h}$ when the critical hole solution branches off the β phase.

There is another set of solutions of Eq. (2.8). As is known [29], if the domain size X_0 exceeds a certain value, the latter branches off the line of γ states and can be viewed as small-amplitude modulations on the top of the γ states [$G \rightarrow \Delta\varphi(\xi_\gamma, h)$; see condition (2.9) and Fig. 1]. The thermodynamic criterion for the bifurcation of monotonic solutions with the unit aspect ratio ($N=1$) from the line of γ states takes the form

$$\varphi^*_{\xi\xi} + \kappa \left[\frac{\pi}{X_0} \right]^2 = 0 \tag{2.46}$$

and defines the bifurcational value $\Delta\theta^*$ of the supercooling of the α state that coresponds to this point. Here and below functions with an asterisk should be taken at the bifurcation point $\gamma^* = \{\xi^*_\gamma, T^*\}$. These solutions may represents IES's in *very fine* particles. To study their locus on the equilibrium phase diagram we introduce a small parameter ε as a measure of the distance from the bifurcation point, Eq. (2.46), so that

$$T = T^* + ET_0\varepsilon^2 , \tag{2.47a}$$

and expand the solution of Eq. (2.8) in powers of ε:

$$\xi = \xi^*_\gamma + \varepsilon u_1(x) + \varepsilon^2 u_2(x) + \varepsilon^3 u_3(x) + \cdots . \tag{2.47b}$$

The singular perturbation analysis of Eq. (2.8) shows [29] that

$$u_1 = u_0 \cos\left[\frac{\pi x}{X_0} \right] ,$$
$$u_0^2 = 24ET_0 \frac{\varphi^*_{\xi\xi\xi}\varphi^*_{\xi T} - \varphi^*_{\xi\xi T}\varphi^*_{\xi\xi}}{3\varphi^*_{\xi\xi\xi\xi}\varphi^*_{\xi\xi} - 5(\varphi^*_{\xi\xi\xi})^2} . \tag{2.48}$$

In order to find the supercooling of the parent state that leads to the creation of the IES (2.47) we shall calculate its total energy. Utilizing Eq. (2.27), the conservation of energy, Eq. (2.4), takes the form

$$\frac{\Delta\theta - \Delta\theta^*}{\varepsilon^2} = r(M^* - 1) + \frac{T^*}{L}\left[\varphi^*_{\xi\xi T} - \frac{\varphi^*_{\xi\xi\xi}\varphi^*_{\xi T}}{\varphi^*_{\xi\xi}} \right] \times \frac{u_0^2}{4} + \cdots . \tag{2.49}$$

Equations (2.48) and (2.49) give the expression for the harmonic wave amplitude $A = \varepsilon u_0$ of the IES, Eq.(2.47), versus the initial supercooling $\Delta\theta$ of the α state beyond the bifurcation value $\Delta\theta^*$. For the system of the size $\Lambda = 5$ with the free energy, Eq. (2.20), and parameters $E = 0.5, Q = 2$ ($r = 0.25$) this amplitude is depicted in Fig. 4 (thick line) together with the average value of the OPF (transformation fraction f, solid line):

$$f = \xi^*_\gamma - \varepsilon^2 \left[ET_0 \frac{\varphi^*_{\xi T}}{\varphi^*_{\xi\xi}} + \frac{\varphi^*_{\xi\xi\xi}}{\varphi^*_{\xi\xi}} \frac{u_0^2}{4} \right] + \cdots . \tag{2.50}$$

If $\Delta\theta < \Delta\theta^*$ the γ state stays globally stable (AS) and disintegration does not occur. Thus there is a range of supercoolings of the α state $\Delta\theta_{\alpha\gamma} \le \Delta\theta \le \Delta\theta^*$ around the instability point of this state $\Delta\theta = r$ where the entropy of the AS is larger than that of any other state. In this range of supercoolings the AS is a phase and may be observed, which gives one a unique opportunity to study the convex-up regions of the free energy.

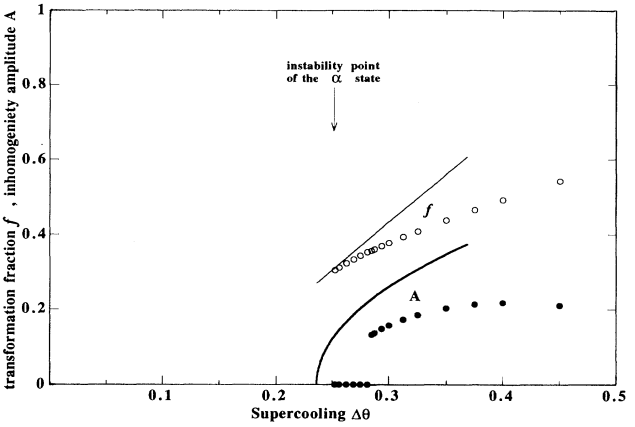

FIG. 4. Inhomogeneity amplitude A and transformation fraction f of a harmonic wave vs supercooling $\Delta\theta$ for the system with $E = 0.5$, $Q = 2$, and $\Lambda = 5$. Analytic results are represented by solid (f) and thick (A) lines. Results of numerical simulation for the system with $R = 4$ below the instability point of the α state are depicted by open circles for the transformation fraction f and solid circles for the inhomogeneity amplitude A.

The calculations of entropies of different equilibrium states versus their energies are summarized in Fig. 5 where entropies of the α state, Eq. (2.24), β state, Eq. (2.25), γ state (AS), Eq. (2.28), and IES, Eq. (2.37), are depicted as functions of the dimensionless initial supercooling $\Delta\theta$ of the α state of the system with $Q = 1$, $E = 0.25$, and $\Lambda = 400$. The product β phase has larger entropy than the parent α phase for $\Delta\theta_{\alpha\beta} \approx 0.4$. But both of them

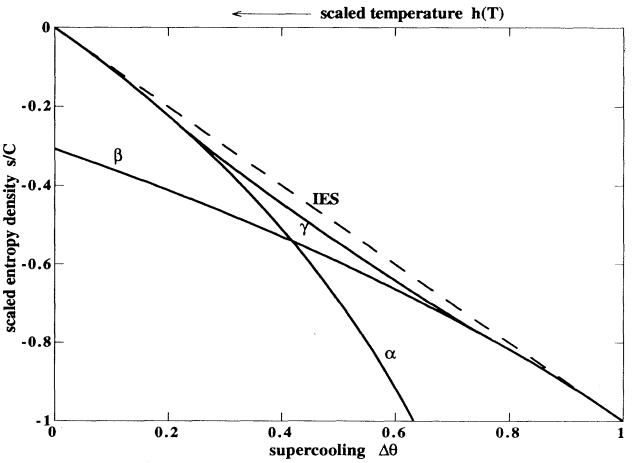

FIG. 5. Scaled entropy densities s/C of equilibrium homogeneous α, β, and γ states (heavy lines) and average entropy density of the inhomogeneous state (IES, dashed line) of the system with $E = 0.25$, $Q = 1$, and $\Lambda = 400$ as functions of the dimensionless initial supercooling $\Delta\theta$ of the α state.

are unstable (have smaller entropy) against the AS, which branches off the α state at $\Delta\theta_{\alpha\gamma}\approx 0.25$ and off the β state at $\Delta\theta_{\beta\gamma}\approx 0.75$. In a large system ($\Lambda=400$) for supercoolings $\Delta\theta_{\alpha w}<\Delta\theta<\Delta\theta_{\beta w}$ the greatest entropy has the $\mathcal{J}=\{f,\Delta h\}$ of the aspect ratio one, and transformation should go in the direction of disintegration into a mixture of parent and product phases separated by the 1D domain wall. This is also true in 2D and 3D cases, because a curved interface has more surface energy and this state should have less entropy than the 1D state with the same energy.

In Fig. 6 the criterion (2.46), together with the analogous criteria for the "critical nucleus" and domain-wall solutions, is depicted in the plane $(\Lambda,\Delta\theta)$ for a system with the free energy (2.20), $Q=1$ and $E=0.25$. In a large particle ($\Lambda\geq 50$) supercooling of the α phase above $\Delta\theta_{\alpha w}$ leads to the apperance of the IES of a domain-wall type on the equilibrium phase diagram with the transformation fraction f, which obeys Eq. (2.36). Below $\Delta\theta_{\alpha w}$ the transformation does not occur and the parent phase remains globally stable (not only metastable). Cooling the α phase deeper than $\Delta\theta_{\beta w}$ leads to the appearance of the homogeneous β phase on the equilibrium state diagram. Moreover, if $\Delta\theta_{\beta w}<\Delta\theta<1$, then the globally stable β phase is superheated above the equilibrium temperature. For smaller particles ($\Lambda\leq 20$), the first IES appears on the phase diagram after supercooling to $\Delta\theta_{\alpha c}$ and looks more like the critical nucleus, which may transfer to a domain-wall-type solution for deeper cooling and to the superheated β phase for still deeper cooling. The latter transition may occur through the "critical-hole"-type solution. In very fine particles ($\Lambda\leq 8$), cooling of the α state first causes appearance of the AS ($\Delta\theta_{\alpha\gamma}=0.221$) with the bifurcation of a harmonic modulation for further cooling deeper than $\Delta\theta^*$. For example, in a fine particle of the size $\Lambda=5$ the IES with a small amplitude of modulation branches off the line of AS's at the bifurcational point $\Delta\theta^*=0.265$. Thus the homogeneous AS, which is designated by an open circle in Fig. 2, is *an absolutely stable phase* of this particle ($\Lambda=5$) supercooled for $0.221\leq\Delta\theta\leq 0.265$. From Fig. 5 notice that the entropy versus energy function of this phase is nonconvex because this is not a bulk phase, but is possible in confined geomtries only. A stable AS may also appear in such a particle for large supercoolings, but the parent state is deeply below the instability point for these supercoolings, which may not be attainable in physical systems. In platelets thinner than $\min\Lambda=\pi\sqrt{2}\approx 4.4$ [see Eq. (2.46)] the AS is absolutely stable below the supercooling $\Delta\theta_{\alpha\gamma}$ (i.e., does not decompose into IES's).

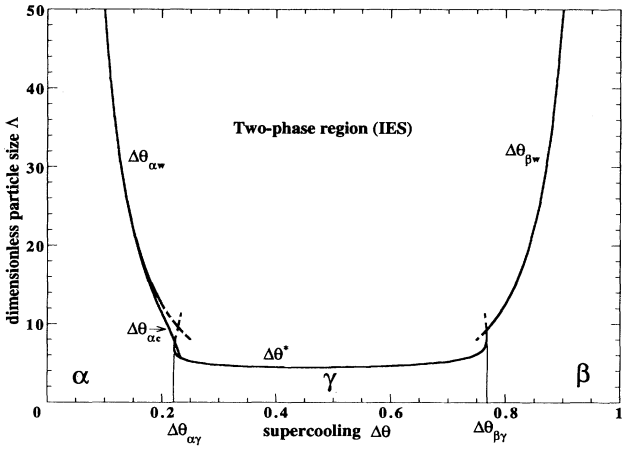

FIG. 6. Equilibrium state diagram of the adiabatically insulated system with $E=0.25$ and $Q=1$. Regions of global stability of the HES's (α, β, and γ phases) are separated from the region of global stability of the IES (two-phase region) by the equilibrium phase boundaries $\Delta\theta_{\alpha w}$ [Eq. (2.39)], $\Delta\theta_{\beta w}$ [Eq. (2.40)], $\Delta\theta_{\alpha c}$ and $\Delta\theta^*$ [Eq. (2.46)]. The dashed lines are invalid continuations of the above equilibrium lines into the two-phase region and are artifacts.

These criteria show the global stability boundaries of HES's and the energy band for the two-phase region (IES) on the equilibrium state diagram. The mathematically exact solution of the stability problem for IES conceivably would give us an envelope of these lines $\Delta\theta_{\alpha w},\Delta\theta_{\beta w},\Delta\theta_{\alpha c},\Delta\theta^*$, but should not differ strongly from the diagram depicted in Fig. 6.

III. EARLY STAGES OF DECOMPOSITION OF UNSTABLE STATES

Thermodynamic analysis (local and global) gives the stability condition of the equilibrium states only with respect to static fluctuations and does not fully describe the physical origin of transformation mainly because it assumes little about the evolutionary processes in a system. The evolution of a thermodynamic system in disequilibrium is accompanied by processes of ordering field relaxation and heat redistribution. For the system where the heat flux can be written in the form $(-\lambda\nabla T)$ the heat transport equation is given by [9]

$$C\frac{\partial T}{\partial t}=\nabla(\lambda\nabla T)-\left[\frac{\partial w}{\partial\xi}-\kappa\nabla^2\xi\right]\frac{\partial\xi}{\partial t}\ ,$$
$$C\equiv\left[\frac{\partial w}{\partial T}\right]_{\xi}=-T\left[\frac{\partial^2\varphi}{\partial T^2}\right]_{\xi}\ , \tag{3.1}$$

where $\lambda\geq 0$ is the thermal conductivity. This equation couples to the relaxation equation for the OPF evolution:

$$\frac{1}{\gamma}\frac{\partial\xi}{\partial t}=-\frac{\partial\varphi}{\partial\xi}+\kappa\nabla^2\xi\ , \tag{3.2}$$

where the coefficient $\gamma>0$ determines the characteristic time of relaxation. Different dynamical regimes of evolution in the vicinity of equilibrium states are governed by the modulus M, Eq. (2.7), which is responsible for *interactions* between energy and OPF modes, and by the ratio $R=\lambda/C\gamma\kappa$ of thermal diffusivity λ/C and interfacial mobility $\gamma\kappa$, which represents kinetic properties of the system [14].

The linear (normal modes) and weakly nonlinear dynamical analysis of HES's of the general system described by Eqs. (3.1) and (3.2) is addressed in [12] and shows that the dynamical criterion of linear stability of an infinite system ($X_0\rightarrow\infty$) takes the form of the in-

equality (2.3), i.e., $M<0$, which differs from the local thermodynamic one for an adiabatic system and coincides with that of an isothermal one [see Eq. (2.7) and the explanations below]. The latter is also true for an IES. This discrepancy between criteria of stability occurs because the normal-mode perturbations in general do not satisfy the energy consrvation requirement, Eq. (2.4), but satisfy the conditions of the microcanonical ensemble [30]. Thus adiabatic and isothermal systems have the same stable HES's (phases), because their dynamical criteria of linear stability coincide. In the unstable region there always exists a band of modes with the cutoff wave number $k_c=\sqrt{-\bar{\varphi}_{\xi\xi}/\kappa}$, which destabilize the HES even if its adiabatic modulus is positive. From Eq. (2.20) one can see that $k_c^{\alpha}=\sqrt{-h}/\delta$ for the unstable α state. This critical excitation of the unstable α state below the instability point has the half-period $l_c^{-}=\pi/k_c^{\alpha}=\pi\delta/\sqrt{-h}$ and is *complementary* to the critical nucleus with the half-width l_c^{+} above the instability point, because both have vanishing growth rates. In Fig. 3 both widths $l_c^{\pm}$ are depicted as functions of h and diverge when $h\to 0\pm 0$.

In a finite 1D system which satisfies the boundary conditions (2.12) only linear modes with wave numbers $k_{N,\Lambda}=\pi N/X_0$ are permitted, where the aspect ratio is $N=0,1,2,\ldots$, and only those with $k_{N,\Lambda}<k_c$ can grow. Thus for HES's with positive adiabatic modulus (e.g., AS of Sec. II) the dynamical condition of marginal stability takes the form $k_{1,\Lambda}=k_c$ or

$$\bar{\varphi}_{\xi\xi}+\kappa k_{1,\Lambda}^2=0 \tag{3.3}$$

because the uniform mode is neutral $\beta(k_{0,\Lambda})=0$ [12]. Applying Eq. (3.3) to the γ state one can see that the stability of this state in a small particle is possible because there are no wave modes permitted in the unstable region. Comparing Eq. (3.3) with Eq. (2.46) we infer that for small size systems the linear dynamic stability criterion *coincides* with that of the global thermodynamic stability criterion.

The linear analysis enables us to assess the influence of nonisothermal effects in an open system. Given the isothermal (Dirichlet-type) boundary conditions the inner thermal fluctuations are important for the dynamics if the amplification rate of the permitted mode $\beta(k_{N,\Lambda})$ differs from that for the completely isothermal system. As this difference is the largest for the first mode with the wave number $k_{1,\Lambda}$ (the uniform mode is prohibited for the isothermal boundry conditions) the criterion of insignificance of thermal effects takes the form

$$\frac{\beta_{\rm iso}(k_{1,\Lambda})-\beta(k_{1,\Lambda})}{\beta_{\rm iso}(k_{1,\Lambda})}\ll 1 . \tag{3.4a}$$

Analysis of the dispersion relation (see Eq. (7) in [12]) shows that this condition is size dependent and yields

$$M\ll\begin{cases}1 \text{ for } X_0\gg\pi/k_c\\ R \text{ for } X_0\approx\pi/k_c\end{cases} . \tag{3.4b}$$

For the α state of the system with the free energy (2.20) $M=0$, which according to the above-described criterion excludes any significance of thermal effects around this state, while for the γ state

$$M_{\gamma}=\frac{\omega(\xi_{\gamma})T}{2\Omega r T_0} \tag{3.5}$$

and nonisothermal effects are significant if the parameter r is small (e.g., surface tension is small).

The nonlinear dynamics near the limit of linear stability of the HES ($\bar{\varphi}_{\xi}=0$) can be expected to differ in cases of various parameters M and R. To examine the nonlinear development of unstable long waves we introduce a small parameter ε which determines the departure from the instability point ($\bar{\varphi}_{\xi\xi}=0$):

$$\bar{\varphi}_{\xi\xi}\sim\varepsilon^2,\quad \bar{\varphi}_{\xi T}\sim\varepsilon,\quad \bar{T}\sim\varepsilon^{-1} . \tag{3.6}$$

As the growing long and sluggish waves are small, we rescale disturbances $\Delta T\sim\varepsilon^3,\Delta\xi\sim\varepsilon^2$ and spatio-temporal coordinates $\mathbf{X}=\varepsilon\mathbf{x},\tau=\varepsilon^3 t$ of the system (3.1) and (3.2). Analysis shows [12] that as a result we obtain the nonlinear Cahn-Hilliard equation for the OPF evolution:

$$\frac{\partial\xi}{\partial t}=\frac{\lambda}{\bar{T}\bar{\varphi}_{\xi T}^2}\nabla^2\left[\left[\frac{\partial\varphi}{\partial\xi}\right]_{\bar{T}}-\kappa\nabla^2\xi\right] . \tag{3.7}$$

If the scaling $\bar{T}\sim\varepsilon^{-1}$ in (3.6) does not hold ($M\sim 1$), then for a small ratio $R=\varepsilon$ the temporal coordinate should be scaled at $\tau=\varepsilon^2 t$ and disturbances $\Delta T\sim\varepsilon^3$, $\Delta\xi\sim\varepsilon^2$ obey the quasiadiabatic system

$$\begin{aligned}&\frac{1}{\gamma}\frac{\partial\xi}{\partial t}=-\left[\left[\bar{\varphi}_{\xi\xi}-\frac{\bar{\varphi}_{\xi T}^2}{\bar{\varphi}_{TT}}\right]\Delta\xi+\tfrac{1}{2}\bar{\varphi}_{\xi\xi\xi}(\Delta\xi)^2\right]+\kappa\nabla^2\xi ,\\ &\bar{\varphi}_{TT}\Delta T+\bar{\varphi}_{\xi T}\Delta\xi=0 ,\end{aligned} \tag{3.8}$$

which is equivalent to Eq. (3.2) where the isothermal modulus is replaced by the adiabatic modulus.

For a large ratio $R=\varepsilon^{-1}$ the temporal coordinate of the system (3.1) and (3.2) should be scaled as $\tau=\varepsilon t$, moduli as $\bar{\varphi}_{\xi\xi}\sim\bar{\varphi}_{\xi T}\sim\varepsilon,\bar{\varphi}_{TT}\sim 1(M\sim\varepsilon)$, and disturbances as $\Delta T\sim\varepsilon^2,\Delta\xi\sim\varepsilon$. In this case equations decouple and we obtain the governing quasi-isothermal system:

$$\begin{aligned}&\frac{\partial\xi}{\partial t}=-\gamma\left[\frac{\partial\varphi}{\partial\xi}\right]_{\bar{T}} ,\\ &C\frac{\partial T}{\partial t}=\lambda\nabla^2 T+\bar{T}\left[\frac{\partial^2\varphi}{\partial\xi\partial T}\right]_{\bar{T}}\frac{\partial\xi}{\partial t} .\end{aligned} \tag{3.9}$$

The resuts of the linear [12] and nonlinear study of the HES stability can be summarized in the parameter space (M,R) as represented in Fig. 7. The uniform mode is the fastest growing mode if $0<M<(1+R)^{-1}$ [the interaction modulus is small and the adiabatic modulus is strongly negative, case (a) of Fig. 7]. This is similar to the isothermal system with the only difference that the uniform mode stability is determined by the adiabatic modulus instead of the isothermal one. If the thermal diffusivity is much weaker than the interfacial mobility ($R\sim\varepsilon$) and interaction is not small ($M\sim 1$), Eqs. (3.8) hold and imply that ordering modes are "slaved" by energy modes and, as a result, the transformation is quasiadi-

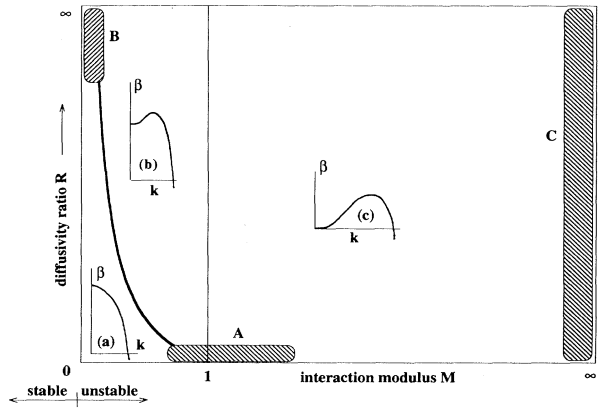

FIG. 7. Instability diagram in the plane (M,R). Hatched areas are the regions of validity of the quasiadiabatic Eq. (3.8), A; quasi-isothermal Eq. (3.9), B; and Cahn-Hilliard Eq. (3.7) of strong correlations, C.

abatic (hatched region A of Fig. 7). If $(1+R)^{-1}<M<1$ [the adiabatic modulus is still negative, case (b) of Fig. 7] the fastest mode has finite wave number and the uniform mode ($k=0$) grows also. For strong thermal diffusivity ($R\sim\varepsilon^{-1}$) and weak interaction ($M\sim\varepsilon$) Eqs. (3.9) apply, wihich means that the ordering process dominates the heat redistribution and the transformation is quasi-isothermal (hatched region B of Fig. 7). For $M>1$ [the interaction modulus is not small and the adiabatic modulus is positive, case (c) of Fig. 7] the wave number of the fastest mode is finite, but the uniform mode is neutral. Thus over this range of conditions the HES is unstable with respect to the continuous modulation of the OPF. For large interaction modulus $M\sim\varepsilon^{-1}$, growing modes obey the nonlinear Cahn-Hillard equation (3.7) with strong correlation of energy and ordering modes (hatched region C of Fig. 7). A large coefficient $\Gamma=\lambda/\overline{T}\overline{\varphi}^2_{\xi T}\sim\varepsilon^{-1}$ is independent of the relaxation constant γ of Eq. (3.2), which means that such a decomposition is totally controlled by heat transfer. We note that an equation analogous to Eq. (3.7) can be derived when the conservation of energy is replaced by the conservation of matter.

The above-described results of dynamic (Sec. III) and thermodynamic (Sec. II) stability analysis allow us to characterize early and ultimate stages of the unstable α-state decomposition during a first-order phase transition. While the process starts as an isothermal one ($M=0$ for the α state) it may later develop short-range instabilities with rather fine structure due to gradual release of latent heat. Eventually the system should reach the more uniform equilibrium state. To more fully examine the completion of microstructure formation, we have chosen to numerically simulate the transformation process. Simulation of the dynamical system of Eqs. (3.1), (3.2), and (2.20) was carried out for ξ and h in the spatiotemporal coordinates scaled with the characteristic space δ and time $\tau=(\gamma a)^{-1}$ intervals. The original problem (for zero biasing field) has seven internal parameters (C,L,T_0, a,κ,λ,γ), an initial temperature T_α, and a size of the system X_0. After the scaling we obtain three dimensionless internal parameters: E,Q,R, a dimensionless initial supercooling $\Delta\theta$, and a dimensionless size of the system Λ. In this scaling, parameter E is a measure of the surface energy relative to the latent heat of transformation. In Sec. IV results are presented for systems with different values of these parameters. First we discuss the transformation process for small particles (small Λ) of systems with $E=0.5$, different parameters Q and R, and different initial conditions $\Delta\theta$. Then we give the results of simulation of initial and late-time stages of transformation in large-size systems with $\Lambda=400$, $Q=1$, and varying E, $\Delta\theta$, and R.

Simulation starts from the parent state which consists of "thermal fluctuations" superimposed on a microstructureless unstable state $\alpha=\{\xi_\alpha=0,h_\alpha<0\}$ (see Fig. 2). The role of thermal fluctuations has been substantially elucidated in the literature. Thermal fluctuations help the system to surmount the barrier for the transition from a weakly metastable state and may also smooth out the critical point. For the transition from an unstable state thermal fluctuations affect significantly the half-completion time of transformation. In the present simulation thermal fluctuations in initial conditions were imitated by a random function with zero mean and mean square $\langle\Delta\xi^2\rangle\approx\langle\Delta h^2\rangle\approx10^{-4}$ and were "turned off" during the calculations in order to study the dynamic properties of the simulating system. The transformation fraction f (2.11) and the total entropy S, Eq. (2.5), were measured, and the conservation of the total energy (enthalpy) W, Eq. (2.4), was checked because of the nonconservative fully explicit numerical scheme employed. Energy was usually conserved better than within 1%. When "entropy change" due to the numerical "thermal flux" outside the system $\Delta S=\Delta W/T$ was larger than that due to irreversible processes inside the system computations were interrupted. Also in numerical "experiments" with an advanced growth stage the dimensionless front velocity v and width l_f were measured:

$$V\frac{\tau}{\delta}\equiv v=\Lambda\frac{\Delta f}{\Delta t},\quad \frac{X_f}{\delta}\equiv l_f=\left[\max\frac{\Delta\xi}{\Delta x}\right]^{-1},$$

where V and X_f are dimensional front velocity and width, respectively. For the system with $Q=0.25$, $E=0.5$, $R=0.1$, and $\Delta\theta=2.02(h_\alpha=-0.01)$ the values of $V=0.91$ and $l_f=4.086$ were obtained in the simulation. For the same parameter values, a study of a stationary moving traveling wave (Fig. 5 of [14]) gives the velocity 0.918, which is in very good agreement with the present result. The front width l_f coincides within the "experimental" error with the analytical estimate of the domain wall thickness, Eq. (2.14b). Note that for the free energy (2.20) the front width is independent of temperature. The comparison of these results helped us to choose parameters of the grid: $\Delta x=0.4,\Delta t=0.05$. So far only 1D simulation has been performed, employing a personal computer.

IV. RESULTS OF SIMULATIONS

To study the mechanism of decomposition of the unstable α state simulations for the system of small size

have been carried out first. In such a system only a few modes have positive amplification rates and the most unstable of them is the uniform mode because the interaction modulus is vanishing for this state [$M=0$, case (a) in Fig. 7]. Therefore the system initially smoothes out tempeature and ordering field fluctuations and, depending upon the structure of the latter, drags towards one of the HES's. The HES $\gamma=\{\xi_\gamma<0, h=2\xi_\gamma\}$ was metastable (linearly stable) and the system remained there for the time of simulation. In the system of length $\Lambda=5$ with parameters $R=4$ and $Q=2$ the AS $\gamma=\{0<\xi_\gamma<1, h=2\xi_\gamma\}$ appeared and did not decompose for supercoolings $\Delta\theta<0.285$ ($h_\alpha>-0.14$), which proves its global stability in this range of supercoolings. For larger values of $\Delta\theta$ the stable OPF distribution appeared to be modulated by a harmonic wave of a small amplitude. In Fig. 4 this amplitude A and transformation fraction f, together with the analytical results, Eqs. (2.48)–(2.50), are depicted as functions of $\Delta\theta$ and give the local supercritical bifurcation structure from homogeneous to periodic solutions. The theoretical value of the bifurcation point [there are no permitted wave modes $k_{N,\Lambda}$ in the unstable interval $0<k<k_c^\gamma$, case (c) in Fig.7] is $\Delta\theta^*\approx 0.236$. The discrepancy between analytical and numerical results is caused by the higher-order terms omitted in Eqs. (2.48)–(2.50).

When the system of length $\Lambda=10$ with parameters $R=5$ and $Q=5$ was supercooled up to $\Delta\theta=0.111(h_\alpha=-0.11)$, it arrived at the AS $\gamma=\{\xi_\gamma=0.164, h_\gamma=0.328\}$ and stayed there for some time. Further evolution of the system passed through a modulation with the wave number $k_{1,\Lambda}=0.314$ of the AS [Fig. 8(a)] with strong correlation of temperature and ordering fields. The wave number of the fastest linear growth mode for the AS of this system $k_m^\gamma=0.320$ [see Eq. (9) of [12]] is very close to $k_{1,\Lambda}$. Later modulations gave rise to the isothermal nonlinear IES [Fig. 8(a)], which had the form of a critical nucleus. In Fig. 8(b) the time dependences of the transformation fraction f, average energy w, and entropy s densities for this system are represented. After the incubation period of ~ 60 the system bursts and the transformation fraction increases to $f\approx 0.164$, which corresponds to the AS. For the next 60 time units the transformation fraction remained unchanged in spite of the rapidly growing amplitude of modulations, which is quite typical for conserved fields, described by Eq. (3.7). The transformation fraction decreased during the nonlinear process of domain formation. Total energy was conserved, the total entropy of the system increased in time and had a terracelike form: horizontal plateaus alternated with steps as a result of growth and modulation.

For $Q=1$, $R=1$, $\Lambda=25$, and $\Delta\theta=0.505(h_a=-0.01)$ the first modulation of the AS $\gamma=\{\xi_\gamma=0.679, h_\gamma=1.358\}$ appeared with $k_{3,\Lambda}=0.378$, which was very close to the fastest one with $k_m^\gamma=0.384$. In the late stages the structure *coarsened* to the wave number $k_{2,\Lambda}=0.253$ (Fig. 9). The transformation fraction did not change during modulations, but was nonmonotonic in the coarsening process. Coarsening is a strongly nonlinear effect which was not incorporated in our weakly nonlinear analysis of Sec. III. For $\Lambda=50$ the first modulation of the HES appeared with $k_{1,\Lambda}=0.063$, but was exceeded soon by the modulation with $k_{5,\Lambda}=0.314$, which had larger amplification rate.

In the system with $Q=0.8, R=5$, $\Lambda=20$, and $\Delta\theta>0.656(h_\alpha\le -0.05)$ transformation starts as a linear modulation of the α state with the wave number $k_{1,\Lambda}=0.157$ and growing amplitude [case (a) of Fig 7]. By the time ~ 200, an almost isothermal nonlinear state reminiscent of the "critical hole" was established in the system as a transient (Fig. 10). In the range of supercool-

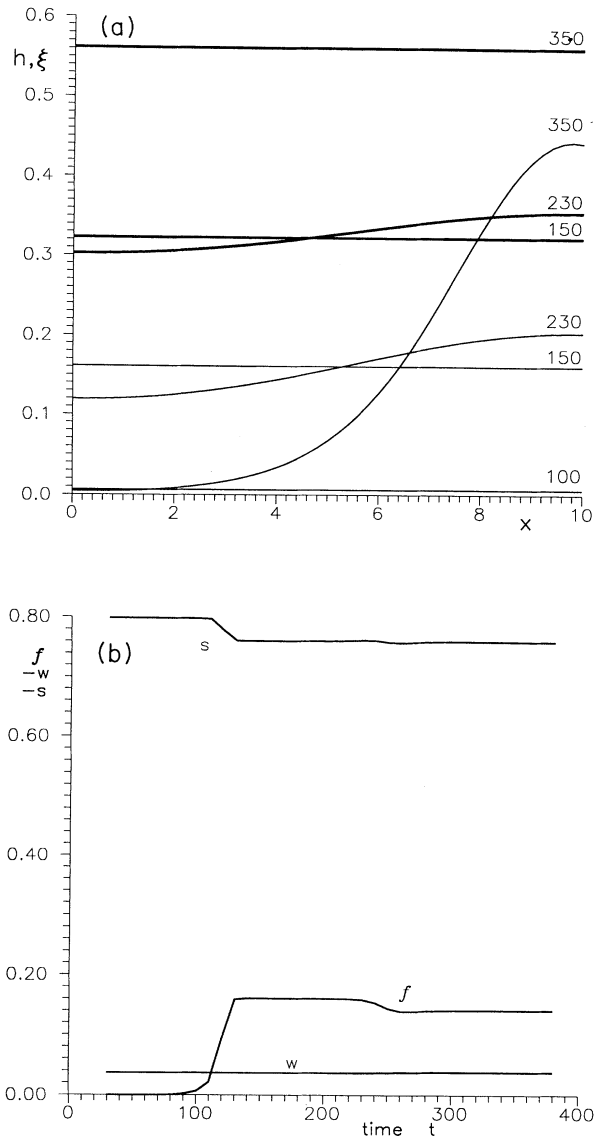

FIG. 8. Evolution of the system with $Q=5$, $R=5$, $\Lambda=10$, and $\Delta\theta=0.111$. (a) Scaled temperature h (heavy lines) and OPF ξ (solid lines) distributions for consequent moments of time (numbers on the lines). (b) Time dependence of the transformation fraction f, average entropy s, and energy w densities.

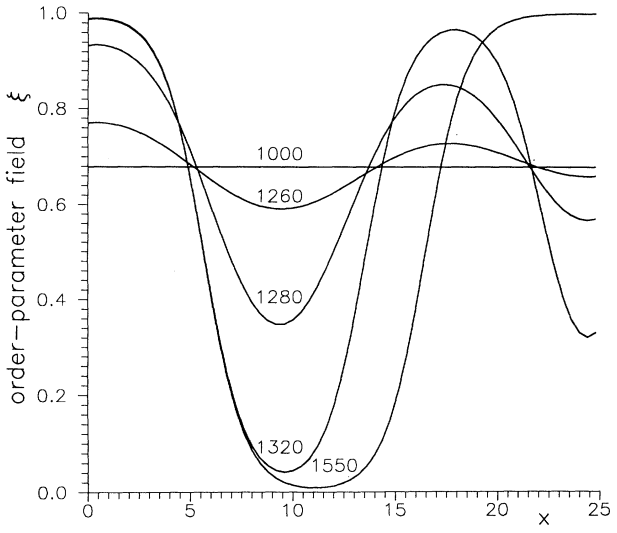

FIG. 9. Evolution of the OPF distribution ξ for the system with $Q=1$, $R=1$, $\Lambda=25$, and $\Delta\theta=0.505$. Numbers on the lines denote moments of time.

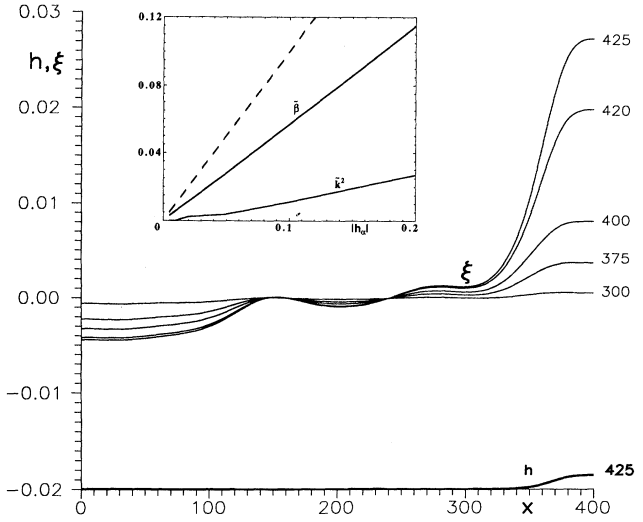

FIG. 11. Distributions of scale temperature h (heavy line) and OPF ξ (solid lines) on initial stages of evolution of the system with $h_\alpha=-0.005$ and $\Lambda=400$. Numbers on the lines denote moments of time. Inset: the square of wave number $\tilde{k}^2$ and amplification rate $\tilde{\beta}$ (heavy lines) vs the initial degree of instability $|h_\alpha|$. The dashed line depicts the amplification rate of the uniform perturbation ($k=0$) and the square of the cutoff wave number ($\beta=0$).

ings $0.675 \le \Delta\theta \le 0.781$ this transient existed for a very long time, $\sim 10\,000$. Eventually the β state with substantial superheating ($h_\beta > 1$) appeared as a result of transformation.

The numerical simulation results for transformation processes in small particles are in good agreement with analytical predictions of their equilibrium state diagrams based on the entropy calculations of Sec. II and the linear and nonlinear dynamical description of Sec. III.

For large-size systems with $\Lambda=400$, $Q=1$, and a small degree of instability ($|h_\alpha| \ll 1$) early stages passed almost completely isothermally: a short-term transient smoothed out the intial fluctuations and turned the system into a slightly modulated uniform unstable state with the modulation of a particular wave number $\tilde{k}$ and amplification rate $\tilde{\beta}$ (Fig. 11). As the distance from the instability point $|h_\alpha|$ gets smaller this wave mode becomes longer and slower. This is reflected in the inset of Fig. 11, where $\tilde{k}^2$

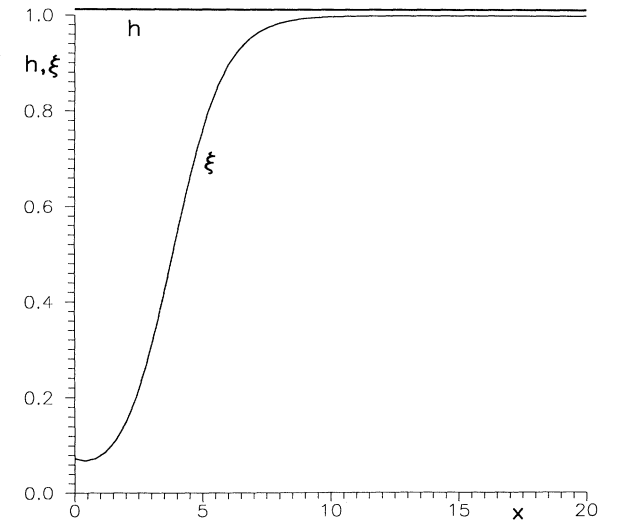

FIG. 10. Scaled temperature h and OPF ξ distributions for the system with $Q=0.8$, $R=5$, $\Lambda=20$, and $\Delta\theta=0.781$ at $t=5000$ (the "critical hole" solution).

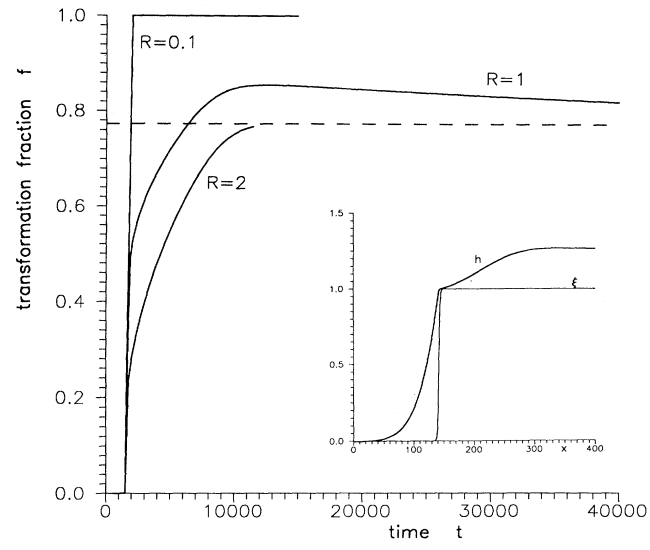

FIG. 12. Evolution of the transformation fraction f of the system with $E=0.769$, $\Delta\theta=0.773$, $\Lambda=400$, and different values of the diffusivity ratio R. Inset: scaled temperature h and OPF ξ distributions in the system with $R=1$ at $t=3500$.

and $\tilde{\beta}$ are depicted as functions of $|h_\alpha|$. At the instability point ($h_\alpha=0$) the modulation occupies the whole domain (the correlation length is infinite) and the transition proceeds extremely slowly (critical slowing down). This picture correlates qualitatively with the linear dynamic stability analysis of Sec. III.

In later stages the OPF grows rapidly in amplitude and evolves into a *nonclassical nucleus* with the same wave number $\tilde{k}$ growing at one of the boundaries (surface) of the system (Fig. 11). The temperature field becomes strongly nonuniform and the evolution depends essentially upon values of parameters E, Q, and R. In the system that does not have the AS [e.g., $E=0.769$, $\Delta\theta=0.773$ ($h_\alpha=-0.005$)] the OPF amplitude of the nucleus grows rapidly towards the β state and, after an incubation period of 1500, the system creates a symmetric *front* which separates parent and product phases. The formation of a front finishes the stage of barrierless decomposition and initiates a stage of *growth*. For the diffusivity ratio $R=2$, after the short-term quasistationary transient, the Stefan regime of growth with monotonically decaying velocity and expanding thermal field ahead of the front is set up in the system (Fig. 12). The system evolves towards global stability in a single-domain form. For $R=1$ the front moves in the Stefan regime towards the opposite side of the box (Fig. 12, inset), gains 86% of the transformation at $t\approx 12\,000$, and then turns back leaving behind a *recovered parent phase* at the temperature very close to the equilibrium point. The process goes further very slowly, approaching by the time $t\approx 40\,000$ an almost

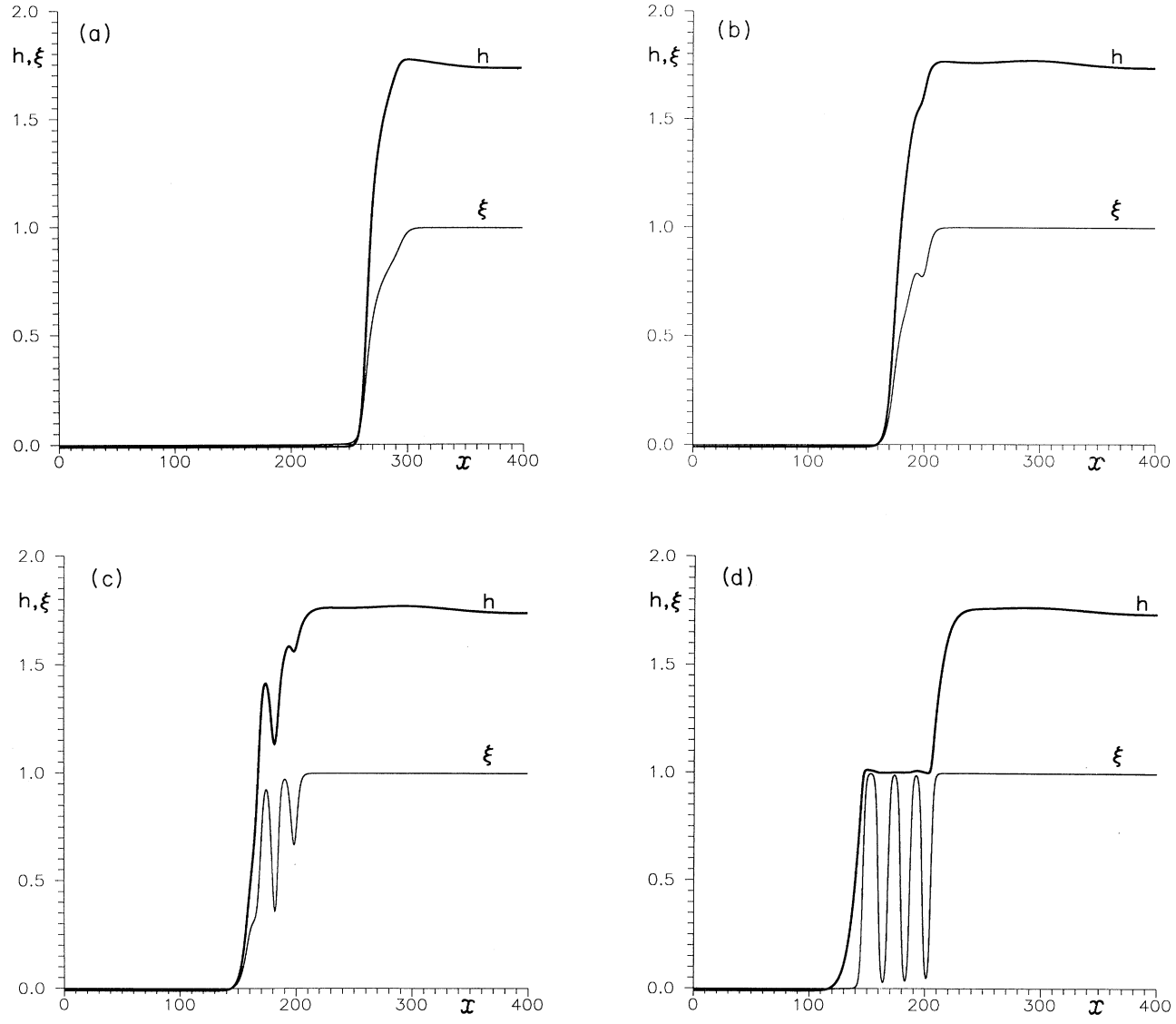

FIG. 13. Evolution of the system with $E=0.555$, $R=1$, and $\Delta\theta=0.561$. Heavy lines, scaled temperature distributions h; solid lines, OPF distributions ξ. (a) $t=1000$; (b) $t=1250$; (c) $t=1300$; (d) $t=1400$.

completely isothermal state with 78% of the product phase (Fig. 12), which is very close to the equilibrium fraction for this system obtained from Eq. (2.36). Here 9% of the ultimate state's parent phase was recovered. Thus one can say that because of relatively high speed of transformation the front "oveshoots" and then "comes back" to the truly equilibrium state. For the system with $R=0.1$ on the stage of growth the stationary traveling wave with $v=0.77$ (heat-trapping regime) was established, because for this system the critical supercooling for heat trapping is $\Delta\theta_{tr}\approx 0.5$ and this regime is allowed: $\Delta\theta_{tr}<\Delta\theta<1$ [$\Delta\theta_{tr}=\theta_l+1$; see Eqs. (4.22) and (4.24) in [14]]. By the time ~ 2000, the front reaches the opposite side of the box, the uniform completely transformed β state with $h_\beta=1.295$ is ultimately attained, and the system never reaches the globablly stable two-phase IES with a domain wall. In this "experiment" the system did not exhibit the stage of recovery and eventually approached the *adiabatically metastable* β state ($T_\beta>T_0$) because the overshooting was too strong. Similar evolution takes place for the systems with $Q\le E$, but here from Eq. (2.23) one can obtain that $h_\beta=h_\alpha+Q/E<1$, i.e., the product phase temperature is below the equilibrium point and the β state is globally stable.

The transition from quasistationary to the Stefan regime does not necessarily happen smoothly in time. In Fig. 13 the consequent stages of evolution of the thermodynamic system with $E=0.555$, $R=1$, and $\Delta\theta=0.561$ are depicted. By the time ~ 1000, a nonsymmetric front forms which is more elongated into the superheated β

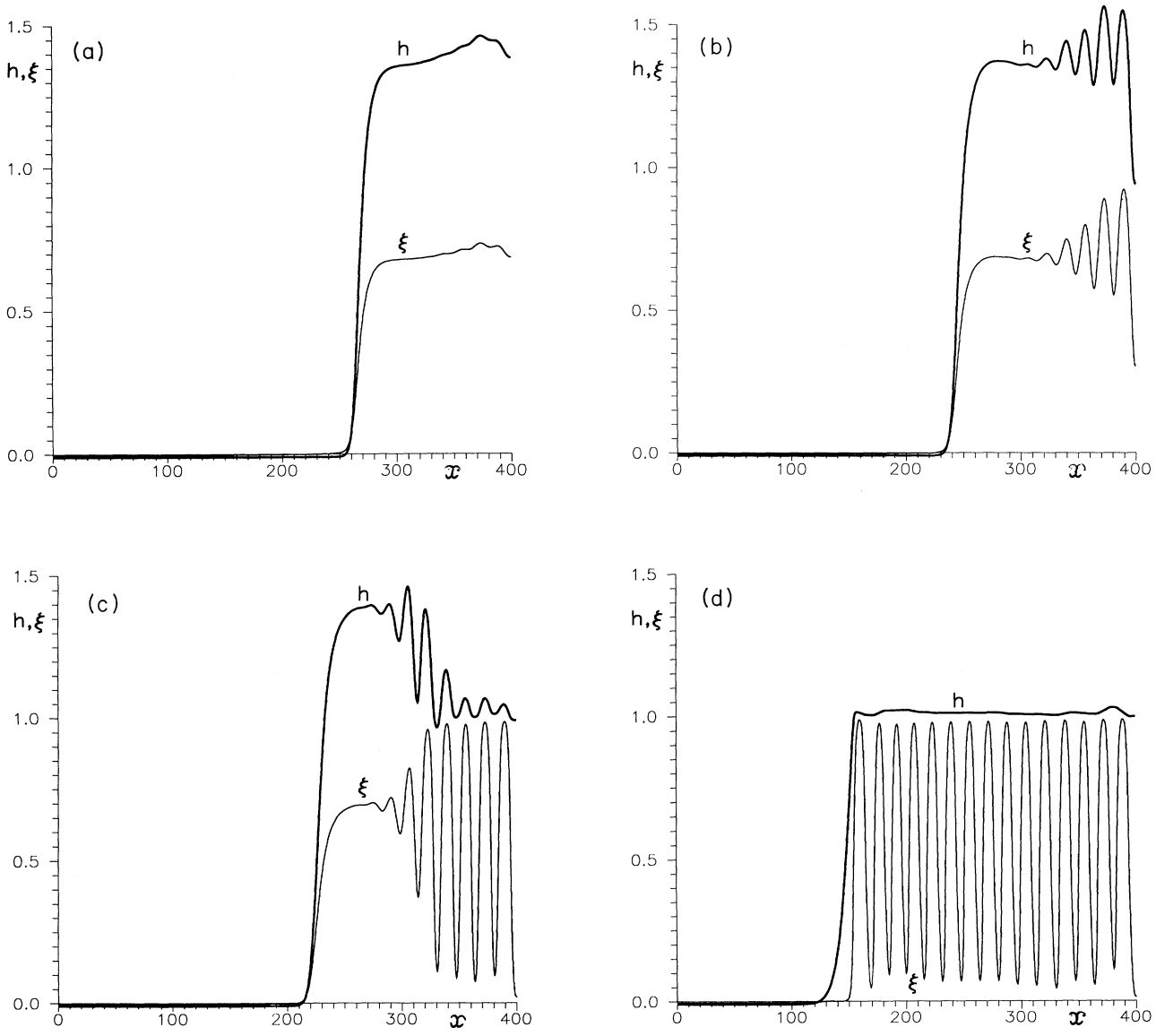

FIG. 14. Modulation mechanism in the early stages of the evolution of the system with $E=0.5$, $R=1$, and $\Delta\theta=0.505$. Heavy lines, scaled temperature distributions h; solid lines, OPF distributions ξ. (a) $t=1000$; (b) $t=1050$; (c) $t=1100$; (d) $t=1400$.

state than into the supercooled α state and moves in the quasistationary heat-trapping regime [Fig. 13(a)]. At $t \approx 1250$ [Fig. 13(b)] the front splits because the heat-trapping regime for this system is not permitted ($\Delta\theta < \Delta\theta_{tr} \approx 0.997$) and modulation appears behind the front. Newly transformed product phase breaks down into domains rather quickly [Fig. 13(c)] and by $t \approx 1400$ a perfect symmetric front propagating in the Stefan regime forms in the system with a domain microstructure behind it [Fig. 13(d)]. For $E = 0.625$ the same modulation appeared on the front, but happened to be unstable and was washed out when the Stefan regime was set up. For $E = 0.671$ this modulation was nucleated ahead of the front, ripened to the complete domain with a symmetric front moving again in Stefan regime. The breakdown into domains and creation of new interfaces helps to eliminate almost completely the overshooting and recovery.

The breakdown into domains may have different variants. For the system with $E = 0.5$, $R = 1$, and $\Delta\theta = 0.505$ ($h_\alpha = -0.01$) this process happens faster and takes place simultaneously with the front formation (Fig. 14). After the incubation period of ~ 1000, a front separating the AS $\gamma = \{\xi_\gamma = 0.679, h_\gamma = 1.358\}$ from the unstable α state was formed. Shortly after that a long-wavelength modulation with $k_n \approx 0.1$ [Fig. 14(a)] appears, which may be identified as the mode with $n = 3$, and was overlapped

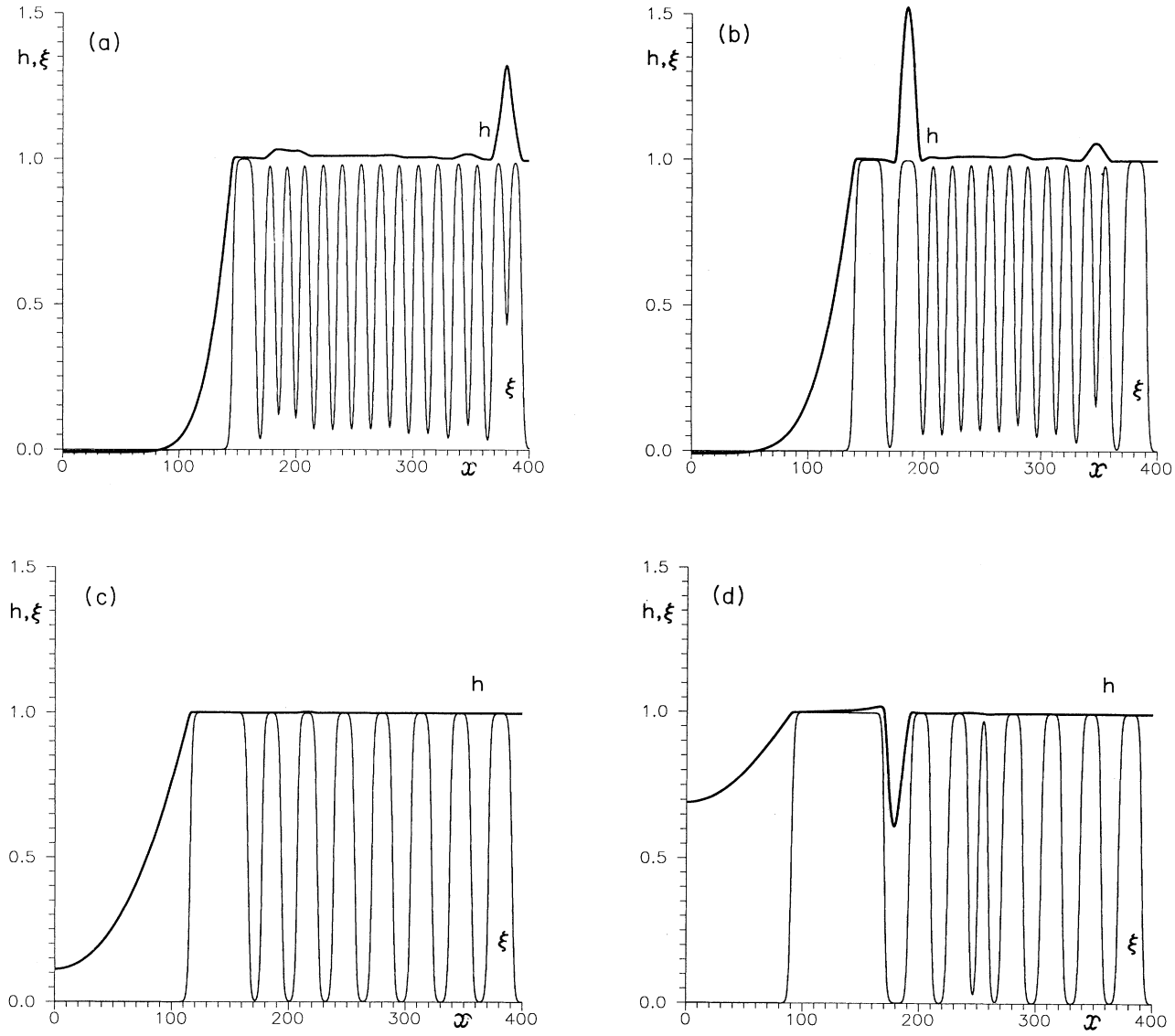

FIG. 15. Coarsening process on the late stages of the evolution of the system with $E = 0.5$, $R = 1$, and $\Delta\theta = 0.505$. Heavy lines, scaled temperature distributions h; solid lines, OPF distributions ξ. (a) $t = 1700$ (coalescence); (b) $t = 2040$ (double coalescence); (c) $t = 4200$ (period doubling); (d) $t = 9100$ (dissolution). The last snapshot was obtained for the same system, but slightly different initial fluctuations.

rapidly by the modulation $n=9$ with $k_9=0.314$ and larger amplification rate [$k_m^{\gamma}=0.384$, case (c) of Fig. 7, also see Eq. (9) of [12]]. On this stage the structure [Fig. 14(b)] has clear signs of these two wave modes, and the decomposition process is described by Eq. (3.7). The appearance of the long-wavelength modulation with the wave number far from the maximal was caused by existence of long-range fluctuations of the AS prior to modulations. By the time $t\approx 1400$ [Fig. 14(d)], the system finishes formation of a symmetric front moving in the Stefan regime and completion of the space behind the front by a domain structure. The fastest modulation, which at first was confined to a small region, resulted in the formation of the domain structure behind the front with the same "zero-time" wave number [Fig. 14(d)], reminiscent of the unstable nonlinear periodic equilibrium solution of Eq. (2.8). Thus one can see that the transformation process may take the form of nucleationlike front creation and subsequent decomposition into domains behind the front resembling spinodal decomposition. The number of interfaces per unit length depends upon the parameter E, which is the ratio of the surface energy and latent heat.

The moving front and decomposed "material" are separated by the region of vanishing temperature and OPF gradients. Therefore further ripening of the structure passed almost absolutely independently in these two adjacent regions and was represented by front advancement (growth) in one of them and coarsening in another. The latter consisted in the disappearance of one of the domains at a time with a full recovery of the β phase in the closest domain [Figs. 15(a) and 15(b)]. At $t\approx 4200$ the coarsened structure again had a quasiperiodic form reminiscent of the unstable equilibrium solution of Eq. (2.8) with the wavelength *twice as large* as that at zero time [Fig. 15(c)]. During coarsening the average domain size (spacing) followed approximately a logarithmic time law. The interaction between coarsening domains went effectively through the temperture field. Two types of coarsening were observed in numerical experiments: *coalescence* and *dissolution*. The former consisted in the straight transformation of the interdomain parent phase and was accompanied by a substantial elevation of the temperature field in this area [Figs. 15(a) and 15(b)], followed by fast relaxation by virtue of domain-wall motion. The coalescing particles were connected by a "neck" [Figs. 15(a) and 15(b)]. The dissolution consisted of the reverse transformation of a domain and was accompanied by a drop of temperature [Fig. 15(d)] and, as a result of the coarsened domain's wall adjustment, temperature recovery to nearly the equilibrium point. Slight variations in the initial conditions may strongly affect coarsening, for instance, significantly retard the process of doubling [Fig. 15(d)]. Eventually the system should come to its global equilibrium state with complete phase separation under a temperature very close to the equilibrium point T_0 [see Eq. (2.38)]. However, after the first period doubling not a single coarsening event had occurred during the next 100 000 time steps of simulation.

For larger supercoolings, when shorter waves are allowed to grow from the very beginning of transformation, the particles "nucleate" closer to each other and coarsening starts from early stages, resembling the Langer-Schwartz mode of transformation [31].

V. DISCUSSION

In this work the thermodynamics and kinetics of first-order transformation from a metastable and weakly unstable state have been studied under conditions of adiabatic insulation. In an isothermal system the homogeneous low-temperature product phase will result after all stages of transformation from the high-temperature parent phase supercooled below the equilibrium point. Even at the equilibrium point, where the last step of coarsening driven by domain-wall expulsion is very slow, eventually a uniform product phase is attained [32]. This is very different from the ultimate state in a large enough adiabatic system where the thermodynamic analysis shows that an initially supercooled (but not hypercooled) parent phase will transform to a mixture of product and parent phases with a temperature very close to the equilibrium point and the transformation fraction dictated by the conservation of energy. The latter is analogous to the lever rule for alloys. The analysis has been made for the 1D structure, but the same inference remains valid in 2D and 3D cases, because a curved interface has more surface energy and this state should have less entropy than the state with the 1D domain wall and the same energy. Hence the creation of an interface (domain wall) is a result of the conservation law in our system. A stable domain wall can also be created in a system obeying the Cahn-Hilliard equation for the conserved order parameter [33]. Conceivably, this is true not only for a domain wall but for creation of stable defects of other types such as line and point defects.

The small-particle phase diagram is more complicated: there is an interval of supercoolings where the transformation does not occur and the parent phase remains globally stable (not metastable). For large supercoolings a partially transformed region appears in the system that grows in size and degree of transformation with increase of supercooling. Strong cooling (but not hypercooling) of the high-temperature parent phase leads to the appearance of the globally stable low-temperature product phase superheated above the equilibrium temperature. For very fine particles with sizes of the order of the interfacial region the intermediate equilibrium (adiabatic) state, which differs from product and parent phases in the degree of transformation and corresponds to the free-energy crest, turns out to be globally stable in a certain range of supercoolings of parent phase in vicinity of the instability point. This unique property of adiabatic systems gives one a chance to study the convex-up segment of the free energy. For larger supercoolings, inhomogeneous equilibrium states modulated by a harmonic wave of small-amplitude branch off the line of adiabatic states. Thus supercooling (or energy) of a small particle does not reflect exactly its tendency towards transformation and the product phase fraction gives one a better idea about the driving force of transformation. This bifurcational picture of a small-particle equilibrium phase diagram

may be relevant for the theory of nanostructural, powder, and composite materials where small particles capable of undergoing a transition are immersed into a poorly conducting matrix, which makes the particle effectively insulated during transformation. The same approach can be applied to small particles of solid solutions where mass conservation replaces the conservation of energy. In this case the present results would predict the appearance of new stable phases with compositions deeply inside the miscibility gap in the equilibrium phase diagram of a small particle.

Numerical simulations were used to track early and late stages of transformation in the 1D system. The calculations verified the theoretical predictions and showed that depending upon initial conditions and internal parameters, the system tends either to completely transform to the stable phase or to form a microstructure consisting of domains of both product and parent phases. Simulations also revealed three mechanisms of domain formation.

(1) "*Nonclassical nucleation.*" In early stages, an isothermal mechanism of correlation of initial fluctuations creates inhomogeneities on the scale of the cutoff wavelength of instability. This mechanism is analogous to nonclassical nucleation which is effective for metastable states just above the instability point and consists in the creation of a diffuse heterophase fluctuation with an amplitude of transformation far below that of the product phase.

(2) *Continuous modulation.* If parameters of the system allow it (e.g., parameter E is small enough), modulations, which emerge from the finite wavelength instability of the adiabatic state, create an almost perfect periodic domain structure in early stages of decomposition. Thus we infer that, for systems with a nonconserved order parameter, decomposition of an unstable state can follow a path of finite-wavelength modulation governed by energy conservation, with a behavior directly analogous to the *spinodal decomposition* of a system with a conserved order parameter. The difference is that for the conserved order-parameter modulations start immediately from the beginning of the process while in our case transformation at first reaches the intermediate equilibrium state along the stable manifold and only then moves along the unstable manifold exhibiting modulations of the order-parameter field. For a weakly metastable system such a mechanism of first-order transformation represents an alternative to nucleation and growth. Achieving the conditions necessary for this mechanism in a specific system will of course depend on the ability to suppress competing nucleation.

(3) *Hybrid transformation.* In the stage of growth, additional domains and their boundaries may appear in the system as the result of a front-splitting instability and a kinetic transition from the stationary to the Stefan regime. Careful study of the equilibrium state diagram of the system shows that front splitting is a result of the continuous modulation mechanism also.

Real transformations that proceed with appreciable speed and a substantial amount of latent heat cannot be truly isothermal. Thus the present analysis may help to understand experimental results of the study of martensitic transformations [34] and solidification [35] in small particles. Solid-liquid transitions in small clusters have been studied previously by the Monte Carlo method [36], showing the solid-liquid coexistence region for the microcanonical ensemble of particles. These results are in good agreement with the present calculations of the equilibrium phase diagram, although the stability of the adiabatic phase was not achieved, presumably because of different boundary conditions. The existence of a mechanism that hinders the martensitic transformation in small particles has been studied in [37] by the molecular-dynamics method. For the boundary conditions that correspond to adiabatic insulation the results indicate the stability of a small particle of the order of nanometers even below the instability point. In the case of a displacive transformation with strain as a nonconserved order parameter, the modulation mechanism (quasimartensitic transformation [18]) may cause the appearance of a periodic platelet structure observed in many experiments. As shown in [12], the modulation process can start even from a high-symmetry parent phase (austenite) if the biasing field b (stress) is applied, because in this case the parent phase symmetry is broken and the interaction modulus M appears to be nonzero from the very beginning of transformation.

The observation of the periodic structures during the order-disorder transition in the Fe-rich Fe-Al alloys [38] may be explained by the above described mechanism: long-range order is a nonconserved parameter that, in principle, excludes the development of modulations during transformation; but being coupled to the conserved concentration field may exhibit the modulation mechanism.

There is a discrepancy between the ultimate state of the system and the fine-grained structure which appears in the early stages of transformation. Two mechanisms help the system to attain a stable equilibrium: growth and coarsening. Growth is a fast mechanism which occurs usually far from equilibrium and may involve a heat-trapping regime with metastable product phase formation. Notice that this regime exists even in an infinitely *large* system, in contrast to the equilbriumal superheating of small particles. In this stage, depending upon the kinetic properties of the system, relaxation towards equilibrium may be accompanied by an overshooting with subsequent recovery of the parent phase and achievement of the globally stable structure or even trapping by a metastable homogeneous state (locally stable, not unstable globally).

Coarsening is a slow mechanism of establishment of the global two-phase equilibrium with a complete phase separation. It is customary to view coarsening as a curvature-driven motion. In this case, there would be no coarsening in the 1D system where all boundaries are flat. In fact, coarsening is driven by the reduction of surface energy which has the form of reduction of the number of domain walls in our system. When the volume fraction of coarsening particles is rather high the coarsening process, which is a result of strong short-range interaction between close particles through the order-parameter field,

takes the form of the sequential doubling of the structural period (spacing). Two types of coarsening may occur: dissolution of a particle, accompanied by a local temperature dip, or coalescence of two neighboring particles, accompanied by the creation and growth of interconnecting neck and strong local elevation of temperature. Both of them eventually lead to a new equilibrium state with the double period.

The system under study is not the only example of period-doubling during coarsening. The evolutionary picture drawn by the results of simulations in a nonequilibriumal system correlates qualitatively with that proposed by Langer [1] for spinodal decomposition. However, the scenario of period doubling requires a different time law of the evolution:

$$\frac{dP}{dt}=\frac{P}{\tau(P)}\ , \tag{5.1}$$

where $\tau(P)$ is the sum of all "unstable" eigenvalues of the state with the period P, which characterizes the decay time of the latter. Operation of this mechanism was observed during numerical simulation of the coarsening stage after the spinodal decomposition in a binary alloy [39]. Numerical simulations of dendritic growth [40] show that the coarsening process of the sidebranch structure during the growth stage also exhibits the mechanism of period doubling which was substantiated by the direct experimental observations of growing dendrites of succinonitrile [41] and ammonium bromide [42]. Thus the mechanism of sequential period doubling is robust for coarsening of systems with a conserved quantity.

Summing up the results of numerical simulation and attempting to describe the scenario of transformation in the functional space one can say that the representative point of our system travels rather quickly from one unstable inhomogeneous equilbrium state to another "less unstable" one (i.e., with longer lifetime), spending much time in the vicinity of the latter, until it reaches the global optimizer and the Lyapunov functional (negative entropy in the present case) attains a minimum. Entropy increase governs pattern formation in an insulated system. The principle of minimum-entropy production does not seem applicable to this strongly nonlinear system. Even slight variations in initial conditions and the system parameters may lead to substantial differences in the kinetic paths toward the ultimate equilibrium state, or even trapping in a metastable state (not allowing the system to attain the global equilibrium, at least in finite time). The results may raise a legitimate question as to why the system generates many interfaces at the beginning (decomposition stage) and slowly eliminates them later (coarsening stage). The answer is in the parameter $E=\sigma/\delta L$. If this parameter is small, it is beneficial to create many "inexpensive" interfaces which helps the system to diffuse the latent heat away. Otherwise, a gradual release of heat in the stage of growth, when a relatively small number of interfaces is involved, becomes favorable.

The present study also enables us to conjecture on the transformation scenario from a weakly metastable state. Initial stages will be similar to that of an isothermal system and consist of the nucleation process which is fully determined by thermal fluctuations, because effects of heat liberation are not essential for the α phase (the interaction modulus is zero). However, evolution of the supercritical nuclei will be very much different from isothermal by virtue of coupling between energy and ordering modes in the region of the γ state because here the interaction modulus does not vanish. This coupling may lead to the pattern formation analogous to that during the unstable state decomposition.

Expansion of the considered problem to 2D and 3D systems will increase the rate of coarsening because of the curvature effect and bring a new issue of morphological stability of growing particles [43], but should not change the scenario of transformation substantially: Initial almost completely isothermal stages do not involve considerable heat fluxes and consist of nucleation-type events. Later, due to the continuous modulation mechanism or morphological front instability, there appears a two-phase "mushy" zone with high density of interfaces (large surface-to-volume ratio), large transformation fraction, and temperature very close to the equilibrium point. The results of the numerical simulation confirm the quasiequilibrium hypothesis of the theory of the mushy zone [44].

VI. CONCLUSIONS

The results of the present study lead us to the following conclusions. (i) The equilibrium phase diagram of an adiabatically insulated system is very much different from the isothermal case. Inhomogeneous states that correspond to complete phase separation may be globally stable under adiabatic conditions while being even locally unstable under isothermal conditions. Stabilization of a domain wall separating parent and product phases is due to the conservation law in our system.

(ii) The conservation law also brings a strong size dependence of the equilibrium phase diagram. For very fine particles the intermediate equilibrium state, corresponding to the free-energy crest, turns out to be globally stable, which is uniquely different from larger particles. This property of small particles potentially gives one a chance to study the upward-convex segments of the free energy.

(iii) There are several mechanisms of the creation of interfaces in our system. In early stages, an isothermal mechanism of correlation of fluctuations creates a diffuse heterophase fluctuation on the scale of the cutoff wavelength of instability. Due to the coupling between nonconservative ordering and conservative energy modes early stages of the unstable state disintegration can follow a path of finite-wavelength modulation directly analogous to a spinodal decomposition. The interaction of this mechanism with the traditional growth can lead to a hybrid mode of transformation which is responsible for the kinetic transition from one growth regime to another.

(iv) Two mechanisms, growth and coarsening, help the system to attain a stable equilibrium; these can proceed simultaneously. Growth is a fast mechanism which occurs usually far from equilibrium and under adiabatic

conditions may involve overshooting and recovery or even a heat-trapping regime with metastable phase formation.

(v) Coarsening is a slow mechanism of establishment of the global two-phase equilibrium with a complete phase separation. Two types of coarsening may occur: dissolution of a domain, accompanied by a local temperature dip, or coalescence of two neighboring domains, accompanied by the creation and growth of an interconnecting neck and strong local elevation of temperature. The coarsening regime in the conditions of high volume fraction exhibits a mechanism of sequential period doubling, which leads to a time law different from that of other coarsening mechanisms.

(vi) The scenario of transformation is characterized by relatively quick hops from one unstable or metastable equilibrium to another one, spending a substantial part of the transformation time in the vicinity of these equilibria. Moreover, different parts of the system may be occupied by different equilbrium states with a transition region between them.

ACKNOWLEDGMENT

This work was supported by the National Science Foundation under Grant No. DMR-8820116 on Mechanism of First-Order Transformations.

[1] J. S. Langer, Ann. Phys. (N.Y.) **65**, 53 (1971).
[2] H. Metiu, K. Kitahara, and J. Ross, J. Chem. Phys. **65**, 393 (1976); in *Fluctuation Phenomena,* edited by E. W. Montroll and J. L. Lebowitz (North-Holland, Amsterdam, 1987), p. 259.
[3] J. W. Cahn, Acta Metall. **9**, 795 (1961); J. W. Cahn and J. E. Hilliard, *ibid.* **19**, 151 (1971).
[4] B. I. Halperin, P. C. Hohenberg, and S.-K. Ma, Phys. Rev. B **10**, 139 (1974).
[5] O. Penrose and P. Fife, Physica D **43**, 44 (1990).
[6] N. S. Fastov, Zh. Eksp. Teor. Fiz. **22**, 487 (1952); A. Z. Patashinsky and I. S. Yakub, *ibid.* **73**, 1954 (1977) [Sov. Phys. JETP **46**, 1025 (1977)]; I. S. Yakub, Fiz. Tverd. Tela (Leningrad) **21**, 524 (1979) [Sov. Phys. Solid State **21**, 310 (1979)].
[7] G. Caginalp, Arch. Ration. Mech. **92**, 207 (1986).
[8] J. B. Collins and H. Levine, Phys. Rev. B **31**, 6119 (1985).
[9] A. Umantsev and A. Roitburd, Fiz. Tverd. Tela (Leningrad) **30**, 1124 (1988) [Sov. Phys. Solid State, **30**, 651 (1988)].
[10] S.-K. Ma, *Modern Theory of Critical Phenomena* (Benjamin, Worcester, MA, 1976), G. Dee, J. D. Gunton, and K. Kawasaki, Prog. Theor. Phys. **65**, 365 (1981); M. San Miguel *et al.*, Phys. Rev. B **23**, 2334 (1981); K. R. Elder *et al.*, *ibid.* **44**, 6673 (1991).
[11] P. C.Fife and G. S. Gill, Physica D **35**, 267 (1989); Phys. Rev. A **43**, 843 (1991).
[12] A. Umantsev and G. B. Olson, Phys. Rev. A **46**, R6132 (1992).
[13] A. Umantsev, Kristallografiya **30**, 153 (1985) [Sov. Phys. Crystallogr. **30**, 87 (1985)]; J. N. Dewyne, S. D. Howison, J. R. Ockendon, and W. Xie, J. Austr. Math. Soc. Ser. B **31**, 81 (1989); M. Marder, Phys. Rev. A **45**, R2158 (1992).
[14] A. Umantsev, J. Chem. Phys. **96**, 605 (1992).
[15] A.Z. Patashinsky and M. V. Chertkov, Fiz. Tverd. Tela (Leningrad) **32**, 509 (1990) [Sov. Phys. Solid State **32**, 295 (1990)]; S.A. Schofield and D. W. Oxtoby, J. Chem. Phys. **94**, 2176 (1991); H. Lowen and J. Bechhoefer; Europhys. Lett. **16**, 195 (1991); H. Lowen, J. Bechhoefer, and L. S. Tuckerman, Phys. Rev. A **45**, 2399 (1992).
[16] J. C. Baker and J. W. Cahn, Acta Metall. **17**, 575 (1969); W. J. Boettinger, S. R. Coriell, and R. F. Sekerka, Mater. Sci. Eng. **65**, 27 (1984).
[17] L. Stodolsky, Phys. Rev. A **39**, 3646 (1989).
[18] M. Cohen, G. B. Olson, and P. C. Clapp, in *Proceedings of the International Conference on Martensitic Transformation* (MIT, Cambridge, MA, 1979), p. 1; G. B. Olson, Mater. Sci. Forum **56-58**, 89 (1990).
[19] L. D. Landau, Phys. Z. Sowjet. **12**, 123 (1937); in *Collected Papers of L. D. Landau,* edited by D. Ter Haar (Gordon and Breach, London, 1967), p. 236.
[20] J. W. Gibbs, *The Scientific Papers* (Dover, New York, 1961), Vol. 1, p. 56.
[21] A. G. Khachaturyan and R. A. Suris, Kristallografiya **13**, 83 (1968) [Sov. Phys. Crystallogr. **13**, 63 (1968)]; A. G. Khachaturyan, *Theory of Structural Transformations in Solids* (Wiley, New York, 1983), p. 117.
[22] W. I. Khan, J. Phys. C **19**, 2969 (1986); P. Winternitz, A. M. Grundland, and J. A. Tuszynski, *ibid.* **21**, 4931 (1988).
[23] A. M. Grundland, E. Infeld, G. Rowlands, and P. Winternitz, J. Phys. Condens. Matter **2**, 7143 (1990), have proven stability of periodic solutions for the *unphysical* free-energy potential that $\Delta\varphi \rightarrow -\infty$ for $\xi \rightarrow \pm\infty$.
[24] P. W. Bates and P. C. Fife, Physica D **43**, 335 (1990), studying dynamic stability of IES, also came to the same conclusion.
[25] L. Kaufman and M. Hillert, in *Martensite,* edited by G. B. Olson and W. S. Owen (ASM International, Materials Park, OH, 1992), p. 41.
[26] Fife and Gill [11] also obtained an exponential deviation of temperature.
[27] S.-K. Chan, J. Chem. Phys. **67**, 5755 (1977).
[28] G. B. Olson and M. Cohen, J. Phys. (Paris) Colloq. **43**, C4-75 (1982).
[29] P. Grindrod, *Patterns and Waves* (Oxford University Press, New York, 1991), p. 24.
[30] R. Kubo, *Statistical Mechanics* (North-Holland, Amsterdam, 1990).
[31] J. S. Langer and A. J. Schwartz, Phys. Rev. A **21**, 948 (1980).
[32] J. Carr and R. L. Pego, in *PDEs and Continuum Models of Phase Transitions,* edited by M. Rascle, D. Serre, and M. Slemrod, Lecture Notes in Physics Vol. 344 (Springer-Verlag, Berlin, 1989), p. 216.
[33] C. M. Elliot and D. A. French, IMA J. Appl. Math. **38**, 97 (1987).
[34] R. E. Cech and D. Turnbull, Trans. AIME **206**, 124 (1956); S. Kajiwara, S. Ohno, and K. Honma, Philos. Mag. A **63**, 625 (1991); M. Lin, G. B. Olson, and M. Cohen, Acta Metall. Mater. **41**, 253 (1993).
[35] Y-W. Kim, H-M. Lin, and T. F. Kelly, Acta Metall. **37**, 247 (1989).

[36] D. J. Wales and R. S. Berry, J. Chem. Phys. **92**, 4473 (1990); H. P. Cheng, X. Li, R. L. Whetten, and R. S. Berry, Phys. Rev. A **46**, 791 (1992).
[37] T. Suzuki and K. Takahashi, Mater. Trans. JIM **33**, 184 (1992).
[38] S. M. Allen and J. W. Cahn, Acta Metall. **24**, 425 (1976).
[39] P. Fife (private communication).
[40] A. Umantsev, V. V. Vinogradov, and V. T. Borisov, Kristallografiya **30**, 455 (1985); *ibid.* **31**, 1002 (1986) [Sov. Phys. Crystallogr. **30**, 262 (1985); *ibid.* **31**, 596 (1986)].
[41] S.-C. Huang and M. E. Glicksman, Acta Metall. **29**, 717 (1981).
[42] A. Dougherty, P. D. Kaplan, and J. P. Golub, Phys. Rev. Lett. **58**, 1652 (1987).
[43] A. Umantsev and S. H. Davis, Phys. Rev. A **45**, 7195 (1992).
[44] V. T. Borisov, Dokl. Akad. Nauk USSR **136**, 583 (1961) [Sov. Phys.—Dokl. **6**, 74 (1961)]; M. G. Worster, in *Interactive Dynamics of Convection and Solidification,* edited by S. H. Davis *et al.* (Kluwer Academic, Dordrecht, 1992), p. 113.